Are We There Yet?

The STAR Collaboration's Critical Evaluation of the Evidence Regarding Formation of a Quark Gluon Plasma in RHIC Collisions

---

Contents

1 Introduction

The Relativistic Heavy Ion Collider was originally sold to the broader physics community and to the funding agencies as the facility needed to enable a meaningful search for the formation of a quark-gluon plasma (QGP) in the laboratory. As we near the end of the fourth successful RHIC running period, it is important to assess the overall quality of the evidence from RHIC experiments for QGP formation. We do so in this document, basing our assessment on results from the first three RHIC runs, as analysis of data collected during run 4 is just beginning. The results from the first three runs are often dramatic, sometimes unexpected, and generally in excellent agreement among the four RHIC experiments (and we utilize results from all of the experiments here). They clearly demonstrate heretofore unobserved behavior for the strongly interacting matter formed during the early collision stages. Does this behavior yet permit a compelling discovery claim for the QGP?

In addressing this question, it is critical to begin by defining clearly what we mean by the QGP, since theoretical expectations of its properties have evolved significantly over the 20 years since the case for RHIC was first made. For our purposes here, we take the QGP to be **a (locally) thermally equilibrated state of matter in which quarks and gluons are deconfined from hadrons, so that color degrees of freedom become manifest over *nuclear*, rather than merely nucleonic, volumes**. In concentrating on thermalization and deconfinement, we significantly omit the following oft-discussed properties from the list we feel are essential for a compelling demonstration.

- We do not demand that the quarks and gluons in the produced matter be non-interacting, as was considered in early conceptions of the QGP. Lattice QCD calculations suggest that such an ideal QGP state may be approached only at temperatures very much higher than that required for the deconfinement transition. Furthermore, RHIC results are certainly not consistent with a non-interacting plasma state. While the absence of interaction would allow considerable simplifications in the calculation of thermodynamic properties of the matter, we do not regard this as an essential feature of color-deconfined matter. In this light, some have suggested [1] that we label the matter we are seeking as the sQGP, for strongly-interacting quark-gluon plasma.
- We do not require evidence of a first- or second-order phase transition, even though most of the experimental signatures originally suggested for the QGP [2] involved searches for sharp changes with collision energy. This relaxation of demands allows for a QGP discovery in a thermodynamic regime beyond a possible critical point, where most modern lattice QCD calculations indeed suggest RHIC collisions will first form the matter. Nonetheless,

such calculations still predict a rapid (but unaccompanied by discontinuities in thermodynamic observables) crossover transition in the bulk properties of strongly interacting matter.

- We do not consider evidence for chiral symmetry restoration to be necessary for a compelling demonstration of the QGP, although most lattice QCD calculations do predict that this transition will accompany deconfinement. If clear evidence for deconfinement can be provided by the experiments, then the search for manifestations of chiral symmetry restoration will be one of the most profound goals of further investigation of the matter's properties, as they would provide the clearest evidence for fundamental modifications to the QCD vacuum, with potentially far-reaching consequences.

The above"relaxation" of demands makes a daunting task even more challenging. Theoretical calculation of the properties of this matter become subject to all the complexities of strong QCD interactions, and hence to the technical limitations of lattice gauge calculations. Even more significantly, these QCD calculations must be supplemented by other models to describe the complex dynamical entry of heavy-ion collision matter into, and exit from, the QGP state. Heavy ion collisions represent our best opportunity to make this unique matter in the laboratory, but we place exceptional demands on these collisions: they must not only produce the matter, but then must serve "pump and probe" functions somewhat analogous to the modern generation of condensed matter instruments, but they must do it all on distance scales of femptometers and a time scale of 10^{-23} seconds!

There are two basic classes of probes at our disposal in heavy ion collisions. In studying electroweak collision products, we exploit their *absence* of final-state interactions (FSI) with the evolving strongly interacting matter, hoping to isolate those produced during the early collision stages and bearing the imprints of the bulk properties characterizing those stages. But we have to deal with the relative scarcity of such products, and the competing origins from hadron decay and interactions during later collision stages. Most of the RHIC results to date utilize instead the far more abundant hadron products, where one exploits (but then must understand) the FSI. It becomes critical to distinguish *partonic* FSI from *hadronic* FSI, and to distinguish both from initial-state interactions and effects of (so far) poorly understood parton densities at very low momentum fractions in the entrance-channel nuclei. Furthermore, the formation of hadrons from a QGP involves soft processes (parton fragmentation and recombination) that cannot be calculated from perturbative QCD and are *a priori* not well characterized (nor even cleanly separable) inside hot strongly interacting matter.

In light of all these complicating features, it is remarkable that the RHIC experiments have already produced results that appear to confirm some of the more striking, and at least semi-quantitative, predictions made on the

basis of QGP formation! Other, unexpected, RHIC results have stimulated new models that explain them within a QGP-based framework. The most exciting results differ markedly from observations at an order of magnitude lower center-of-mass energy, and indeed are somewhat orthogonal to the observations on which a circumstantial case for QGP formation was previously argued at CERN [3]. In order to assess whether a discovery claim is now justified, we must judge the robustness of both the new experimental results and the theoretical predictions they seem to bear out. Do the RHIC data *demand* a QGP explanation, or can they alternatively be accounted for in a hadronic framework? Are the theories and models used for the predictions mutually compatible? Are those other experimental results that currently appear to deviate from theoretical expectations indicative of details yet to be worked out, or rather of fundamental problems with the QGP explanation?

We organize our discussion as follows. In Chapter 2 we briefly summarize the most relevant theoretical calculations and models, their underlying assumptions, limitations and most robust predictions. We thereby try to identify the *crucial* QGP features we feel must be demonstrated experimentally to justify a compelling discovery claim. We divide the experimental evidence into three areas in Chapters 3-5, focusing first on what he have learned about the bulk thermodynamic properties of the early stage collision matter from such measures as flow, and their consistency with thermalization and the exposure of new (color) degrees of freedom. Next we provide an overview of the observations of high-momentum hadron production yields and angular correlations, and what they have taught us about the nature of FSI in the collision matter. In Chapter 5 we focus on open questions for experiment and theory, on predictions not yet borne out by experiment and experimental results not yet accommodated by theory. Finally, we provide in Chapter 6 an extended summary, conclusions and outlook, with emphasis on additional measurements and theoretical improvements that we feel are needed to strengthen any discovery claim. The summary of results in Chap. 6 is extended so that readers already familiar with most of the theoretical and experimental background material covered in Chaps. 2-5 can skip to the concluding section without missing the arguments central to our assessment of the evidence.

2 Predicted Signatures of the QGP

The promise, and then the delivery, of experimental results from the SPS and from RHIC have stimulated impressive and important advances over the past decade in the theoretical treatment of the thermodynamic and hydrodynamic properties of hot strongly interacting matter and of the propagation of partons through such matter. However, the complexities of heavy-ion collisions and of hadron formation still require a patchwork of theories and models to treat the entire collision evolution, and the difficulties of the strong interaction introduce significant quantitative ambiguities in all aspects of this patchwork. In support of a possible compelling QGP discovery claim, we must then identify the most striking qualitative predictions of theory, which survive the quantitative ambiguities, and we must look for a congruence of various observations that confirm such robust predictions. In this chapter, we provide a brief summary of the most important pieces of the theoretical patchwork, their underlying assumptions and quantitative limitations, and what we view as their most robust predictions. Some of these predictions will then be compared with RHIC experimental results in later chapters.

2.1 Features of the Phase Transition in Lattice QCD

The phase diagram of bulk thermally equilibrated strongly interacting matter should be described by QCD. At sufficiently high temperature one must expect hadrons to "melt", deconfining quarks and gluons. The exposure of new (color) degrees of freedom would then be manifested by a rapid increase in entropy density, hence in pressure, with increasing temperature, and by a consequent change in the equation of state (EOS). In the limit where the deconfined quarks and gluons are non-interacting, and the quarks are massless, the (Stefan-Boltzmann) pressure P_{SB} of this partonic state, as a function of temperature T at zero chemical potential (*i.e.*, zero net quark density), would be simply determined by the number of degrees of freedom [4]:

$$\frac{P_{SB}}{T^4} \;=\; [2(N_c^2-1)+\frac{7}{2}N_cN_f]\frac{\pi^2}{90}, \qquad (1)$$

where N_c is the number of colors, N_f the number of quark flavors, and the two terms on the right represent the gluon and quark contributions, respectively. Refinements to this basic expectation, to incorporate effects of color interactions among the constituents, as well as of non-vanishing quark masses and chemical potential, and to predict the location and nature of the transition from hadronic to partonic degrees of freedom, are best made via QCD calculations on a space-time lattice (LQCD).

In order to extract physically relevant predictions from LQCD calculations, these need to be extrapolated to the continuum (lattice spacing $\rightarrow 0$), chiral (actual current quark mass) and thermodynamic (large volume) limits. Computing power limitations have restricted the calculations to date to numbers of lattice points that are still considered marginal from the viewpoint of these extrapolations [4]. The computing cost has also permitted only limited explorations of sensitivity to details of the calculations [4]: *e.g.*, the number and masses of active quark flavors included; the technical treatment of quarks on the lattice; the presence or absence of the $U_A(1)$ anomaly in the QGP state. Additional numerical difficulties have so far plagued calculations at nonzero chemical potential and have complicated the determination of physical quark mass scales for a given lattice spacing [4].

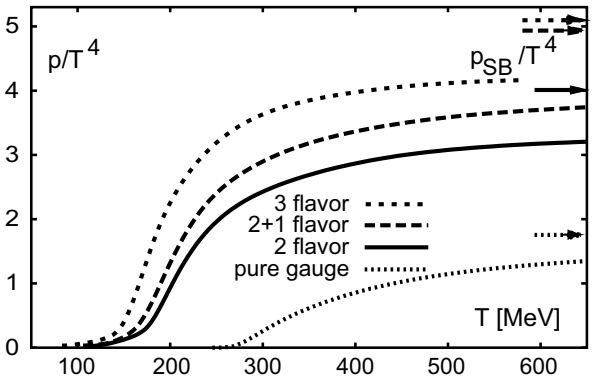

Fig. 1. *LQCD calculation results from Ref. [5] for the pressure divided by T^4 of strongly interacting matter as a function of temperature, and for several different choices of the number of relevant quark flavors. The arrows near the right axis indicate the corresponding Stefan-Boltzmann pressures for the same quark flavor assumptions.*

Despite the technical complications, LQCD calculations have converged on the following predictions:

- There is indeed a predicted transition of some form between a hadronic and a QGP phase, occurring at a temperature in the vicinity of $T_c \simeq 160$ MeV for zero chemical potential. The precise value of the transition temperature depends on the treatment of quarks in the calculation.
- The pressure divided by T^4 rises rapidly above T_c, then begins to saturate by about $2T_c$, but at values substantially below the Stefan-Boltzmann limit (see Fig. 1) [5]. The deviation from the SB limit indicates substantial remaining interactions among the quarks and gluons in the QGP phase.
- Above T_c, the effective potential between a heavy quark-antiquark pair takes the form of a screened Coulomb potential, with screening mass (or inverse screening length) rising rapidly as temperature increases above T_c (see Fig. 2) [6]. As seen in the figure, the screening mass deviates strongly from perturbative QCD expectations in the vicinity of T_c, indicating large non-perturbative effects. The increased screening mass leads to a shorten-

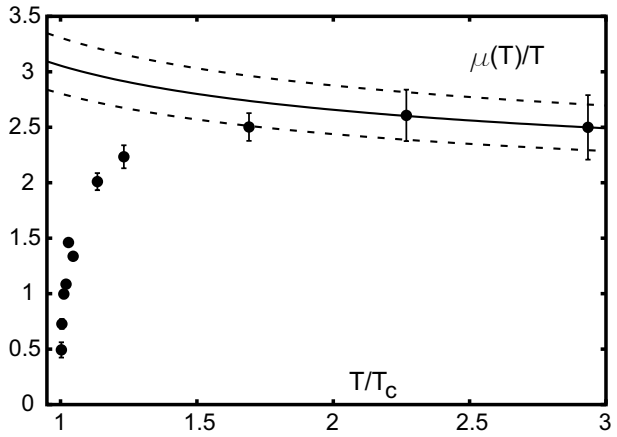

Fig. 2. *Temperature-dependence of the heavy-quark screening mass (divided by temperature) as a function of temperature (in units of the phase transition temperature), from LQCD calculations in Ref. [6]. The curves represent perturbative expectations of the temperature-dependence.*

ing of the range of the $q\overline{q}$ interaction, and to an anticipated suppression of charmonium production, in relation to open charm [7]. The predicted suppression appears to set in at substantially different temperatures for J/ψ $(1.5 - 2.0T_c)$ and ψ' $(\sim 1.0T_c)$ [8].

- In most calculations, the deconfinement transition is also accompanied by a chiral symmetry restoration transition, as seen in Fig. 3 [5]. The reduction in the chiral condensate leads to significant predicted variations in in-medium meson masses. These are also affected by the restoration of $U_A(1)$ symmetry, which occurs at higher temperature than chiral symmetry restoration in the calculation of Fig. 3.
- The nature of the transition from hadronic to QGP phase is highly sensitive to the number of active quark flavors included in the calculation and to the quark masses [9]. For the most realistic calculations, incorporating two light (u, d) and one heavier (s) quark flavor relevant on the scale of T_c, the transition is most likely of the crossover type (with no discontinuities in thermodynamic observables – as opposed to first- or second-order phase transitions) at zero chemical potential, although the ambiguities in tying down the precise values of quark masses corresponding to given lattice spacings still permit some doubt.
- Calculations at non-zero chemical potential, though not yet mature, suggest the existence of a critical point such as that illustrated in Fig. 4 [10]. The numerical challenges in such calculations leave considerable ambiguity about the value of μ_B at which the critical point occurs, but it is most likely above the value at which RHIC collision matter is formed, consistent with the crossover nature of the transition anticipated at RHIC.
- Even for crossover transitions, the LQCD calculations still predict a rapid temperature-dependence of the thermodynamic properties, as revealed in all of the figures considered above.

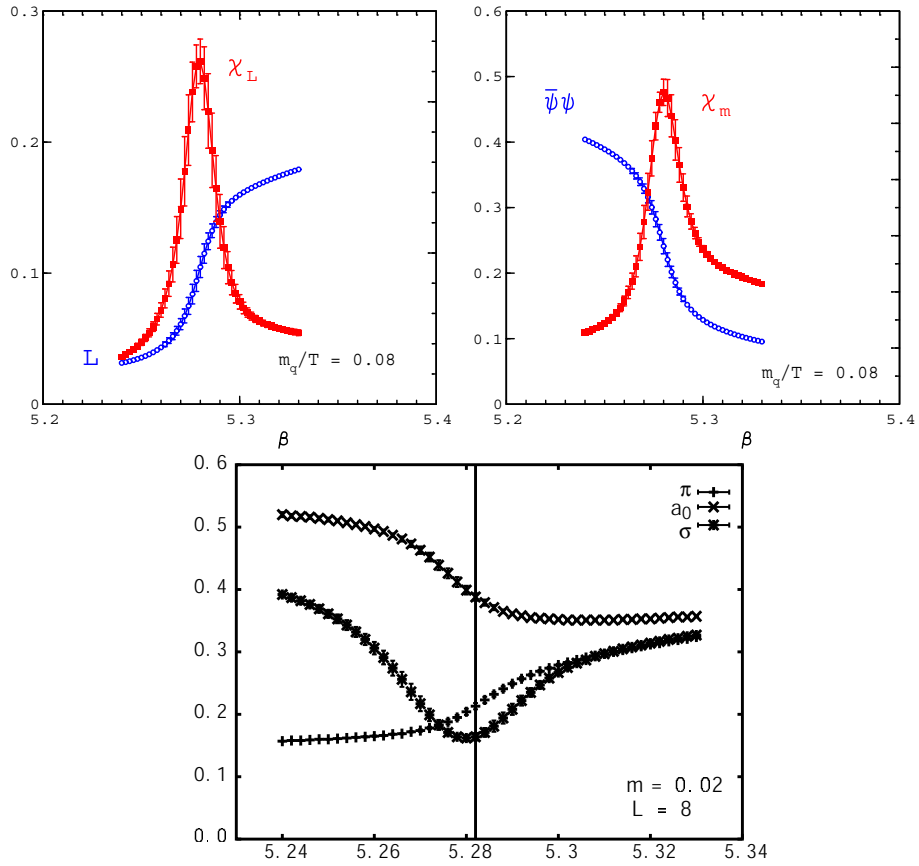

Fig. 3. *LQCD calculations for two dynamical quark flavors [5] showing the coincidence of the chiral symmetry restoration (marked by the rapid decrease of chiral condensate $\langle\overline{\psi}\psi\rangle$ in the upper right-hand frame) and deconfinement (upper left frame) phase transitions. The lower plot shows that the chiral transition leads to a mass degeneracy of the pion with scalar meson masses. All plots are as a function of the bare coupling strength β used in the calculations; increasing β corresponds to decreasing lattice spacing and to increasing temperature.*

2.2 Hydrodynamic Signatures

In order to determine how the properties of bulk QGP matter, as determined in LQCD calculations, may influence observable particle production spectra from RHIC collisions, one needs to model the time evolution of the collision "fireball". To the extent that the initial interactions among the constituents are sufficiently strong to establish local thermal equilibrium rapidly, and then to maintain it over a significant evolution time, the resulting matter may be treated as a relativistic fluid undergoing collective, hydrodynamic flow [11]. The application of hydrodynamics for the description of hadronic fireballs has a long history [12,13]. Relativistic hydrodynamics have been extensively applied to heavy ion collisions from BEVALAC to RHIC [13,14,11], but with the most striking successes at RHIC. The applicability of hydrodynamics at RHIC may provide the clearest evidence for the attainment of local thermal equi-

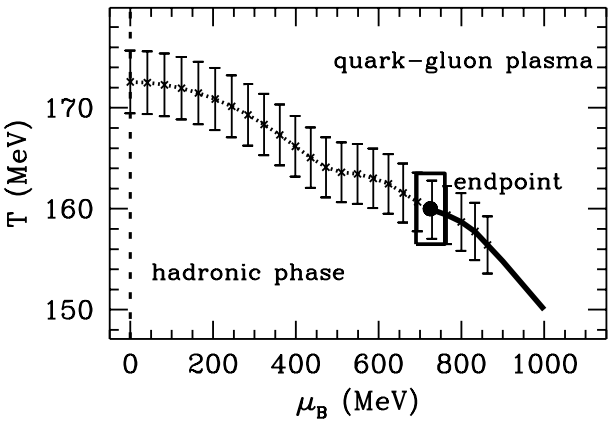

Fig. 4. *Early LQCD calculation results for non-zero chemical potential [10], suggesting the existence of a critical point well above RHIC chemical potential values. The solid line indicates the locus of first-order phase transitions, while the dotted curve marks crossover transitions between the hadronic and QGP phases.*

librium at an early stage in these collisions. The details of the hydrodynamic evolution are clearly sensitive to the EOS of the flowing matter, and hence to the possible crossing of a phase transition during the system expansion and cooling. It is critical to understand how this sensitivity compares with that to other uncertain aspects of the hydrodynamic treatment.

Hydrodynamics cannot be applied to matter not in local thermal equilibrium, hence hydrodynamics calculations must be supplemented by more phenomenological treatments of the early and late stages of the system evolution. These determine the initial conditions for the hydrodynamic flow and the transition to freezeout and final hadron spectra. Since longitudinal flow is especially sensitive to initial conditions beyond the scope of the theory, most calculations to date have concentrated on *transverse* flow, and have assumed longitudinal boost invariance of the predictions [11]. Furthermore, it is anticipated that hadrons produced at sufficiently high transverse momentum in initial partonic collisions will not have undergone sufficient rescatterings to come to thermal equilibrium with the surrounding matter, so that hydrodynamics will be applicable at best only for the softer features of observed spectra. Within the time range and momentum range of its applicability, most hydrodynamics calculations to date have treated the matter as an *ideal*, non-viscous fluid, so that the equations of motion are governed by exact local conservation of energy, momentum, baryon number, etc. The motion of the fluid is then completely determined given the three components of the velocity $\vec{v}$, the pressure (p) and the energy density (e), or any two of $\vec{v}$, p and e together with the equation of state [12].

The EOS in hydrodynamics calculations for RHIC has been implemented using simplified models inspired by LQCD results, though not reproducing their details. One example is illustrated by the solid curve in Fig. 5, connecting an

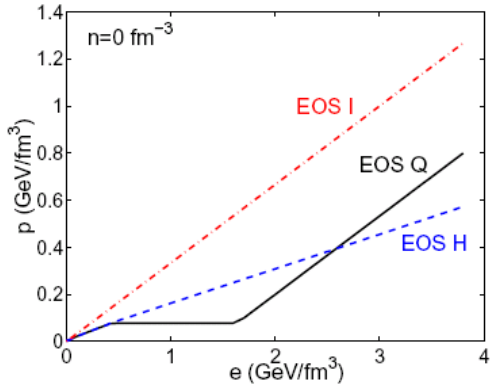

Fig. 5. *Pressure as a function of energy density at vanishing net baryon density for three different equations of state of strongly interacting matter: a Hagedorn resonance gas (EOS H), an ideal gas of massless partons (EOS I) and a connection of the two via a first-order phase transition at T_c=164 MeV (EOS Q). These EOS are used in hydrodynamics calculations in Ref. [11].*

ideal gas of massless partons at high temperature to a Hagedorn hadron resonance gas [15] at low temperatures, via a first-order phase transition chosen to ensure consistency with ($\mu = 0$) LQCD results for critical temperature and net increase in entropy density across the transition [11]. In this implementation, the slope $\partial p/\partial e$ (giving the square of the velocity of sound in the matter) exhibits high values for the hadron gas and, especially, the QGP phases, but has a soft point at the mixed phase [13,11]. This generic softness of the EOS during the assumed phase transition has predictable consequences for the system evolution.

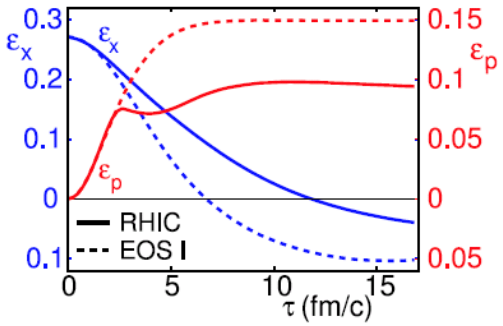

Fig. 6. *Hydrodynamics calculations for the time evolution of the spatial eccentricity ϵ_x and the momentum anisotropy ϵ_p for non-central (7 fm impact parameter) Au+Au collisions at RHIC [11]. The solid and dashed curves result, respectively, from use of EOS Q and EOS I from Fig. 5. The gradual removal of the initial spatial eccentricity by the pressure gradients that lead to the buildup of ϵ_p reflects the self-quenching aspect of elliptic flow. The time scale runs from initial attainment of local thermal equilibrium through freezeout in this calculation.*

In heavy ion collisions, the measurable quantities are the momenta of the produced particles at the final state and their correlations. Transverse flow measures are key observables to compare quantitatively with model predictions in studying the EOS of the hot, dense matter. In non-central collisions, the reaction zone has an almond shape, resulting in azimuthally anisotropic pressure gradients, and therefore a nontrivial elliptic flow pattern. The important feature of elliptic flow is "self-quenching" [13], because the pressure-driven expansion tends to reduce the spatial anisotropy that causes the azimuthally anisotropic pressure gradient in the first place. This robust feature is illustrated in Fig. 6, which compares predictions for the spatial and resulting momentum eccentricities as a function of time during the system's hydrodynamic evolution, for two different choices of EOS [11]. The self-quenching makes the elliptic flow particularly sensitive to earlier collision stages, when the spatial anisotropy and pressure gradient are the greatest. In contrast, hadronic interactions at later stages contribute greatly to the radial flow [16,17].

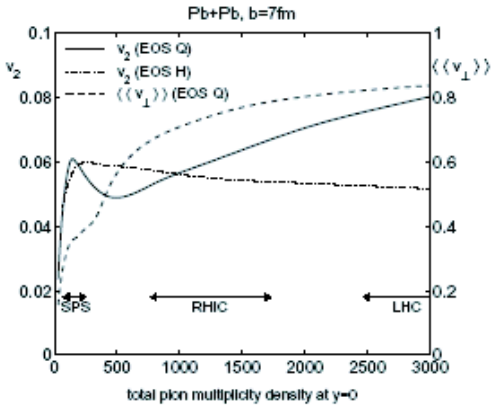

Fig. 7. *Predicted hydrodynamic excitation function of p_T-integrated elliptic (solid curve, left axis) and radial (dashed, right axis) flow for non-central Pb+Pb collisions [19]. The soft phase transition stage in EOS Q gives rise to a dip in the elliptic flow. The horizontal arrows at the bottom reflect early projections of particle multiplicity for different facilities, but we now know that RHIC collisions produce multiplicities in the vicinity of the predicted dip.*

The solid momentum anisotropy curve in Fig. 6 also illustrates that entry into the soft EOS mixed phase during a phase transition from QGP to hadronic matter stalls the buildup of momentum anisotropy in the flowing matter. An even more dramatic predicted manifestation of this stall is shown by the dependence of p_T-integrated elliptic flow on produced hadron multiplicity in Fig. 7, where a dip is seen under conditions where the phase transition occupies most of the early collision stage. Since the calculations are carried out for a fixed impact parameter, measurements to confirm such a dip would have to be performed as a function of bombarding energy. In contrast to early (non-hydrodynamic) projections of particle multiplicities at RHIC (rep-

resented by horizontal arrows in Fig. 7), we now know that the multiplicity at the predicted dip is approximately achieved for appropriate centrality in RHIC Au+Au collisions at full energy. However, comparisons of predicted with measured excitation functions for elliptic flow are subject to an overriding ambiguity concerning where and when appropriate conditions of initial local thermal equilibrium for hydrodynamic applicability are actually achieved. Hydrodynamics itself has nothing to say concerning this issue.

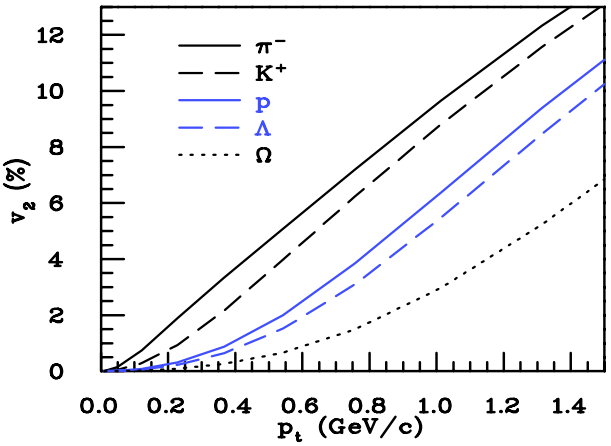

Fig. 8. *Hydrodynamics predictions [20] of the p_T and mass-dependences of the elliptic flow parameter v_2 for identified final hadrons from Au+Au collisions at $\sqrt{s_{NN}}$=130 GeV.*

One can alternatively attain sensitivity to the EOS in measurements for given bombarding energy and centrality by comparing to the predicted dependence of elliptic flow strength on hadron p_T and mass (see Fig. 8). The mass-dependence is of simple kinematic origin [11], and is thus a robust feature of hydrodynamics, but its quantitative extent, along with the magnitude of the flow itself, depends on the EOS [11].

Of course, the energy- and mass-dependence of v_2 can also be affected by species-specific hadronic FSI at and close to the freezeout where the particles decouple from the system, and hydrodynamics is no longer applicable [16,17]. A combination of macroscopic and microscopic models, with hydrodynamics applied at the early partonic and mixed-phase stages and a hadronic transport model such as RQMD [18] at the later hadronic stage, may offer a more realistic description of the whole evolution than that achieved with a simplified sharp freezeout treatment in Figs. 6,7,8. The combination of hydrodynamics with RQMD [17] has, for example, led to predictions of a substantially different, and monotonic, energy-dependence of elliptic flow, as can be seen by comparing Fig. 9 to Fig. 7. This comparison suggests that sensitivity to the late hadronic interaction details is at least as large as that to the mixed-phase EOS. Certainly, these relative sensitivities must be clearly understood in order to interpret agreement between hydrodynamics calculations and measured flow. Flow for multi-strange and charmed particles with small hadronic inter-

action cross sections may provide more selective sensitivity to the properties of the partonic and mixed phases [22,17,23].

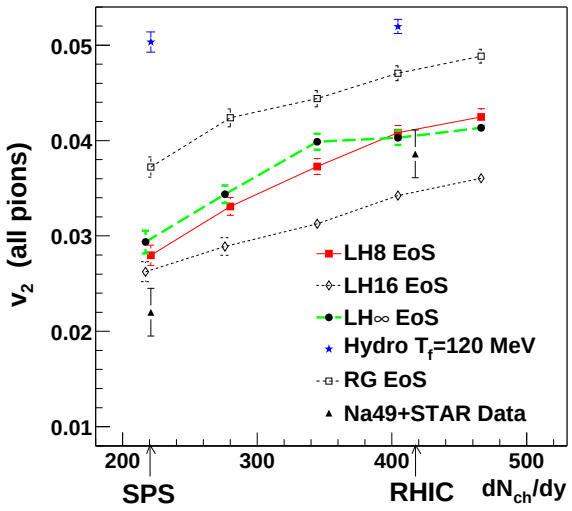

Fig. 9. *Predictions [17] from a hybrid hydrodynamics-RQMD approach for the elliptic flow as a function of charged particle multiplicity in Pb+Pb collisions at an impact parameter $b = 6$ fm. Curves for different choices of EOS (LH8 is most similar to EOS Q in Fig. 7) are compared to experimental results derived [17] from SPS and RHIC measurements. The replacement of a simplified freezeout model for all hadron species with the RQMD hadron cascade appears to remove any dip in v_2 values, such as seen in Fig. 7.*

In addition to predicting one-body hadron momentum spectra as a function of many kinematic variables, hydrodynamic evolution of the matter is also relevant for understanding two-hadron Hanbury-Brown-Twiss quantum correlation functions [24]. From these correlation measurements one can extract information concerning the size and shape of the emitting surface at freezeout, *i.e.*, at the end of the space-time evolution stage treated by hydrodynamics. While the detailed comparison certainly depends on improving models of the freezeout stage, it is reasonable to demand that hydrodynamics calculations consistent with the one-body hadron measurements be also at least roughly consistent with HBT results.

2.3 Statistical Models

The aim of statistical models is to derive the equilibrium properties of a macroscopic system from the measured yields of the constituent particles [26,28]. Statistical models, however, do not describe how a system approaches equilibrium [28]. Hagedorn [15] and Fermi [25] pioneered their application to computing particle production yield ratios in high energy collisions, where conserved

quantities such as baryon number and strangeness play important roles [29]. Statistical methods have become an important tool to study the properties of the fireball created in high energy heavy ion collisions [26,27], where they succeed admirably in reproducing measured yield ratios. Can this success be taken as evidence that the matter produced in these collisions has reached thermodynamic equilibrium? Can the temperature and chemical potential values extracted from such statistical model fits be interpreted as the equilibrium properties of the collision matter?

The answer to both of the above questions is "not necessarily." The essential condition for applicability of statistical models is phase-space dominance in determining the distribution of a system with many degrees of freedom among relatively few observables [25,30], and this does not necessarily reflect thermodynamic equilibration. Indeed, statistical model fits can describe the yields well in p+p, e^+e^- and A+A collisions where thermal equilibrium is thought not to be achieved [26]. In order to distinguish a thermally equilibrated system from one born with statistical phase space distributions, where "temperature" and "chemical potential" are simply Lagrange multipliers [30], it is necessary and sufficient to measure the extensive interactions among particles and to observe the change from canonical ensemble in a small system with the size of a nucleon (p+p, e^+e^-) to grand canonical ensemble in a large system with extended volume (central A+A) [26,29]. The evolution of the system from canonical to grand canonical ensemble can be observed, for example, via multi-particle correlations (especially of particles constrained by conservation laws [30]) or by the centrality dependence of the canonical suppression of strangeness in small systems. The interactions among constituent particles, necessary to attainment of thermal equilibrium, can be measured by collective flow of many identified particles [17,31] and resonance yields [32] according to their hadronic rescattering cross section.

If other measurements confirm the applicability of a grand canonical ensemble, then the hadron yield ratios can be used to extract the temperature and chemical potential of the system [26] at chemical freezeout. The latter is defined as the stage where hadrons have been created and the net numbers of stable particles of each type no longer change in further system evolution. These values place constraints on, but do not directly determine, the properties of the matter when thermal equilibrium was first attained in the wake of the collision. Direct measurement of the temperature at this early stage requires characterization of the yields of particles such as photons that are produced early but do not significantly interact on their way out of the collision zone.

Partons from the colliding nuclei that undergo a hard scattering in the initial stage of the collision provide colored probes for the colored bulk matter that may be formed in the collision's wake. It was Bjorken [33] who first suggested that partons traversing bulk partonic matter might undergo significant energy loss, with observable consequences on the parton's subsequent fragmentation into hadrons. More recent theoretical studies have demonstrated that the elastic parton scattering contribution to energy loss first contemplated by Bjorken is likely to be quite small, but that gluon radiation induced by passage through the matter may be quite sizable [34]. Such induced gluon radiation would be manifested by a significant softening and broadening of the jets resulting from the fragmentation of partons that traverse substantial lengths of matter containing a high density of partons – a phenomenon called "jet quenching". As will be documented in later chapters, some of the most exciting of the RHIC results reveal jet quenching features quite strikingly. It is thus important to understand what features of this phenomenon may distinguish parton energy loss through a QGP from other possible sources of jet softening and broadening.

Two different theoretical approaches to evaluating the non-Abelian radiative energy loss of partons in dense, but finite, QCD matter have been developed [35,36]. They give essentially consistent results, including the non-intuitive prediction that the energy loss varies with the square (L^2) of the thickness traversed through static matter, as a consequence of destructive interference effects in the coherent system of the leading quark and its first radiated gluon as they propagate through the matter. The energy loss is reduced, and the L-dependence shifted toward linearity, by the expansion of the matter resulting from heavy ion collisions. The significant deformation of the collision zone for non-central collisions, responsible for the observed elliptic flow (hence also for an azimuthal dependence of the rate of matter expansion), should give rise to a significant variation of the energy loss with angle with respect to the impact parameter plane. The scale of the net energy loss depends on factors that can all be related to the rapidity density of gluons (dN_g/dy) in the matter traversed.

The energy loss calculated via either of these approaches is then embedded in a perturbative QCD (pQCD) treatment of the hard parton scattering. The latter treatment makes the standard factorization assumption (untested in the many-nucleon environment) that the amplitude for producing a given final-state high-p_T hadron can be written as the product of suitable initial-state parton densities, pQCD hard-scattering amplitude, and final-state fragmentation functions for the scattered partons. Nuclear modifications must be expected for the initial parton densities as well as for the fragmentation functions.

Entrance-channel modifications – including both nuclear shadowing of parton densities and the introduction by multiple scattering of additional transverse momentum to the colliding partons – are capable of producing some broadening and softening of the final-state jets. But these effects can, in principle, be calibrated by complementing RHIC A+A collision studies with p+A or d+A, where QGP formation is not anticipated.

The existing theoretical treatments of the final-state modifications attribute the changes in effective fragmentation functions to the parton energy loss. That is, they assume vacuum fragmentation (as characterized phenomenologically from jet studies in more elementary systems) of the degraded parton and its spawned gluons [34]. This assumption may be valid in the high-energy limit, when the dilated fragmentation time should exceed the traversal time of the leading parton through the surrounding matter. However, its justification seems questionable for the soft radiated gluons and over the leading-parton momentum ranges to which it has been applied so far for RHIC collisions. In these cases, one might expect hadronization to be aided by the pickup of other partons from the surrounding QGP, and not to rely solely on the production of $q\overline{q}$ pairs from the vacuum. Indeed, RHIC experimental results to be described later in this document hint that the distinction between such recombination processes and parton fragmentation in the nuclear environment may not be clean. Furthermore, one of the developed models of parton energy loss [36] explicitly includes energy *gain* via absorption of gluons from the surrounding thermal QGP bath.

The assumption of vacuum fragmentation also implies a neglect of FSI interaction effects for the hadronic fragmentation products, which might further contribute to jet broadening and softening. Models that attempt to account for *all* of the observed jet quenching via the alternative description of hadron energy loss in a hadronic gas environment are at this time still crude [37]. They must contend with the initial expectation of *color transparency* [38], *i.e.*, that high momentum hadrons formed in strongly interacting matter begin their existence as point-like color-neutral particles with very small color dipole moments, hence weak interactions with surrounding nuclear matter. In order to produce energy loss consistent with RHIC measurements, these models must then introduce *ad hoc* assumptions about the rate of growth of these "prehadron" interaction cross sections during traversal of the surrounding matter [37].

The above caveats concerning assumptions of the parton energy loss models may call into question some of their quantitative conclusions, but are unlikely to alter the basic qualitative prediction that substantial jet quenching is a *necessary* result of QGP formation. The more difficult question is whether the observation of jet quenching can also be taken as a *sufficient* condition for a QGP discovery claim? Partonic traversal of matter can, in principle,

be distinguished from effects of *hadronic* traversal by detailed dependences of the energy loss, *e.g.*, on azimuthal angle and system size (reflecting the nearly quadratic length-dependence characteristic of gluon radiation), on p_T (since hadron formation times should increase with increasing partonic momentum [39]), or on type of detected hadron (since hadronic energy losses should depend on particle type and size, while partonic energy loss should be considerably reduced for heavy quarks [39,40]). However, the energy loss calculations do not (with the exception of the small quantitative effect of *absorption* of thermal gluons [36]) distinguish confined from deconfined quarks and gluons in the surrounding matter. Indeed, the same approaches have been applied to experimental results from semi-inclusive deep inelastic scattering [41] or Drell-Yan dilepton production [42] experiments on nuclear targets to infer quark energy losses in *cold*, confined nuclear matter [43]. Thus, the relevance of the QGP can only be inferred from a rapid change in the extent of jet quenching with collision energy [39], or indirectly, from the magnitude of the gluon density dN_g/dy needed to reproduce jet quenching in RHIC collision matter, vis-a-vis that needed to explain the energy loss in cold nuclei. Is the extracted gluon density consistent with what one might expect for a QGP formed from RHIC collisions? To address this critical question, one must introduce new theoretical considerations of the initial state for RHIC collisions.

2.5 Saturation of Gluon Densities

In a partonic view, the initial conditions for the expanding matter formed in a RHIC collision are dominated by the scattering of gluons carrying small momentum fractions (Bjorken x) in the nucleons of the colliding nuclei. Gluon densities in the proton have been mapped down to quite small values of $x \sim 10^{-4}$ in deep inelastic scattering experiments at HERA [44]. When the measurements are made with high resolving power (*i.e.*, with large 4-momentum transfer Q^2), the extracted gluon density $xg(x, Q^2)$ continues to grow rapidly down to the lowest x values measured. However, at moderate $Q^2 \sim$ few $(\mathrm{GeV})^2$, there are indications from the HERA data that $xg(x, Q^2)$ begins to saturate, as might be expected from the competition between gluon fusion ($g + g \to g$) and gluon splitting ($g \to g + g$) processes. It has been conjectured [45–48] that the onset of this saturation moves to considerably higher x values (for given Q^2) in a nuclear target, compared to a proton, and that a QGP state formed in RHIC collisions may begin with a saturated density of gluons.

The onset of saturation occurs when the product of the cross section for a QCD process (such as gluon fusion) of interest ($\sigma \sim \pi\alpha_s(Q^2)/Q^2$) and the areal density of partons (ρ) available to participate exceeds unity [49]. In this so-called Color Glass Condensate region (see Fig. 10), QCD becomes highly non-linear, but amenable to classical field treatments, because the coupling

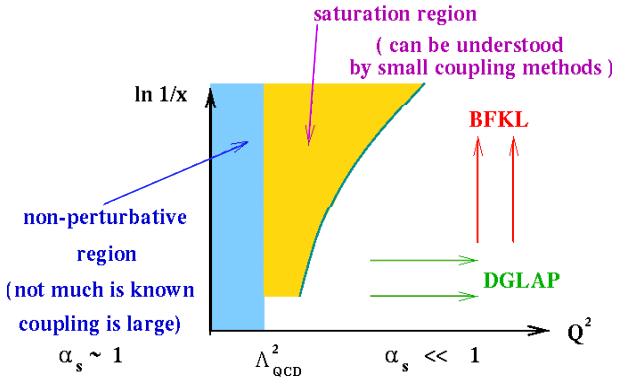

Fig. 10. *Schematic layout of the QCD landscape in $x - Q^2$ space. The region at the right is the perturbative region, marked by applicability of the linear DGLAP and BFKL evolution equations for parton distribution functions. At $Q^2 < \Lambda^2_{QCD}$, the coupling constant is large and non-perturbative methods must be used to treat strongly interacting systems. The matter in RHIC collisions may be formed in the intermediate region, where gluon densities saturate, the coupling is still weak, but very strong color fields lead to non-linear behavior describable by classical field methods. The curve separating the saturation and perturbative regimes sets the saturation scale.*

strength remains weak ($\alpha_s << 1$) while the field strength is large [45–48]. The borderline of the CGC region is denoted by the "saturation scale" $Q_s^2(x, A)$. It depends on both x and target mass number A, because the target gluon density depends on both factors. In particular, at sufficiently low x and moderate Q^2, ρ is enhanced for a nucleus compared to a nucleon by a factor $\sim A^{1/3}$: the target sees the probe as having a longitudinal coherence length ($\ell_c \sim 1/m_N x$) much greater, but a transverse size ($\sim 1/Q^2$) much smaller, than the nuclear diameter. The probe thus interacts coherently with all the target gluons within a small diameter cylindrical "core" of the nucleus. The HERA data [44] suggest a rather slow variation – $xg(x) \propto x^{-\lambda}$, with $\lambda \sim 0.3$ at $Q^2 \sim$ few $(\mathrm{GeV})^2$ – of gluon densities with x at low x. Consequently, one would have to probe a proton at roughly two orders of magnitude lower x than a Au nucleus to gain the same factor growth in gluon densities as is provided by $A^{1/3}$.

Under the assumption that QGP formation in a RHIC collision is dominated by gluon-gluon interactions below the saturation scale, saturation models predict the density of gluons produced per unit area and unit rapidity [45]:

$$\frac{dN}{d^2b dy} = c\frac{N_c^2 - 1}{4\pi^2 \alpha_s(Q_s^2) N_c} Q_s^2(x, A). \tag{2}$$

The x-dependence of the saturation scale is taken from the HERA data,

$$Q_s^2(x) = Q_0^2 (\frac{x_0}{x})^\lambda, \tag{3}$$

and the same values of $\lambda \sim 0.2 - 0.3$ are generally assumed to be valid inside

the nucleus as well. However, the overall saturation scale Q_0^2, as well as the multiplicative factor c above, are typically adjusted to fit observed outgoing hadron multiplicities from RHIC collisions. Once these parameters are fixed, gluon saturation models should be capable of predicting the dependence of hadron multiplicity on bombarding energy, rapidity, centrality and mass number. Furthermore, the initial QGP gluon densities extracted can be compared with the independent values obtained from parton energy loss model fits to jet quenching observations.

While it is predictable within the QCD framework that gluon saturation should occur under appropriate conditions, and the theoretical treatment of the CGC state is highly evolved [45–48], the dependences of the saturation scale are not yet fully exposed by supporting data. Eventual confirmation of the existence of such a scale must come from comparing results for a wide range of high energy experiments from Deep Inelastic Scattering in ep and eA (HERA, eRHIC) to pA and AA (RHIC, LHC) collisions.

2.6 Manifestations of Quark Recombination

The concept of quark recombination was introduced to describe hadron production in the forward region in p+p collisions [50]. At forward rapidity, this mechanism allows a fast quark resulting from a hard parton scattering to recombine with a slow anti-quark, which could be one in the original sea of the incident hadron, or one excited by a gluon [50]. If a QGP is formed in relativistic heavy ion collisions, then one might expect coalescence of the abundant thermal partons to provide another important hadron production mechanism, active over a wide range of rapidity and transverse momentum [51]. In particular, at moderate p_T values (above the realm of hydrodynamics applicability), this hadron production "from below" (recombination of lower p_T partons from the thermal bath) has been predicted [52] to be competitive with production "from above" (fragmentation of higher p_T scattered partons). It has been suggested [53] that the need for substantial recombination to explain observed hadron yields and flow may be taken as a signature of QGP formation.

In order to explain observed features of RHIC collisions, the recombination models [51,52] make the central assumption that coalescence proceeds via *constituent* quarks, whose number in a given hadron determines its production rate. The constituent quarks are presumed to follow a thermal (exponential) momentum spectrum and to carry a collective transverse velocity distribution. This picture leads to clear predicted effects on baryon and meson production rates, with the former depending on the spectrum of thermal constituent quarks and antiquarks at roughly one-third the baryon p_T, and the latter determined by the spectrum at one-half the meson p_T. Indeed, the recombi-

nation model was recently re-introduced in the RHIC context, precisely to explain an anomalous abundance of baryons vs. mesons observed at moderate p_T values [52]. If the observed (saturated) hadronic elliptic flow values in this momentum range result from coalescence of collectively flowing constituent quarks, then one can expect a similarly simple baryon vs. meson relationship [52]: the baryon (meson) flow would be 3 (2) times the quark flow at roughly one-third (one-half) the baryon p_T.

As will be discussed in the following chapters, RHIC experimental results showing just such simple predicted baryon vs. meson features would appear to provide strong evidence for QGP formation. However, the models do not spell out the connection between the inferred spectrum and flow of constituent quarks and the properties of the essentially massless partons (predominantly gluons) in a chirally restored QGP, where the chiral condensate (hence most of the constituent quark mass) has vanished. One may guess that the constituent quarks themselves arise from an earlier coalescence of gluons and *current* quarks during the chiral symmetry breaking transition back to hadronic matter, and that the constituent quark flow is carried over from the partonic phase. But the guesswork implies a leap of faith in inferring the existence of *partonic* collectivity from the success of the quark recombination models.

In addition, it is yet to be demonstrated that the coexistence of coalescence and fragmentation processes is quantitatively consistent with the (near-side) hadron angular correlations observed over p_T ranges where coalescence is predicted to dominate. These correlations exhibit prominent peaks with the angular widths and charge sign ordering characteristic of jets from vacuum fragmentation of hard partons [54]. The coalescence yield might simply contribute to the background underlying these peaks, but one should also expect contributions from the "fast-slow" type of recombination (hard scattered parton with QGP bath partons) for which the model was first introduced, and these could produce charge sign ordering. The latter effects – part of in-medium, as opposed to vacuum, fragmentation – complicate the interpretation of the baryon/meson comparisons and, indeed, muddy the distinction between fragmentation and recombination processes.

Finally, the picture provided by recombination models is distinctly different from ideal hydrodynamics, where velocity (mass) is the crucial physical scale, rather than number of constituent quarks. At low momentum, energy and entropy conservations become a serious problem for quark coalescence, the solution of which requires a dynamical, rather than purely kinematical treatment of the recombination process [52]. It is possible that such partonic dynamics at low momentum can offer a mechanism responsible for the thermodynamical properties of the macroscopic system discussed earlier. But we do not yet have such a unified partonic theoretical viewpoint.

3 Bulk properties

The measured hadron spectra reflect the properties of the bulk of the matter at kinetic freeze-out, after elastic collisions among the hadrons have ceased. At this stage the system is already relatively dilute and "cold". However from the detailed properties of the hadron spectra at kinetic freeze-out, information about the earlier hotter and denser stage can be obtained.

The integrated yields of the different hadron species only change via inelastic collisions. These inelastic collisions cease already (at so-called chemical freeze-out) before kinetic freeze-out. Therefore the yield of the various particle species provides information of an earlier hotter stage.

The transverse momentum distributions of the different particles reflect a random and a collective component. The random component can be identified with the temperature of the system at kinetic freeze-out. The collective component is due to the matter density gradient from the center to the boundary of the fireball created in high-energy nuclear collisions. Interactions among constituents push matter outwards; frequent interactions lead to a common constituent velocity distribution. This so-called collective flow therefore measures the strength of the interactions. The collective flow is additive and thus accumulated over the whole system evolution. At lower energies the collective flow reflects the properties of dense hadronic matter [55], while at RHIC energies a contribution from the partonic phase is expected.

In non-central heavy-ion collisions the initial transverse density gradient has an azimuthal anisotropy that leads to an azimuthal variation of the collective transverse flow velocity. The azimuthal variation of flow is expected to be self-quenching, hence, especially sensitive to the interactions among constituents in the early stage of the collision [56,57], when the system at RHIC energies is anticipated to be well above the critical temperature.

In this section, we review the most important bulk properties measured at RHIC: hadron yield ratios, transverse flow and its azimuthal dependence, and correlation measurements.

3.1 Hadron Yields and Ratios

Mid-rapidity charged hadron densities measured in PHOBOS [58] are plotted in Fig. 11 as a function of collision centrality, as characterized by the number of participating nucleons, N_{part}, inferred from the fraction of the total geometric cross section accounted for in each analyzed bin. Results from Au+Au collisions at $\sqrt{s_{\rm NN}}$= 130 GeV and 200 GeV are shown as open and closed trian-

gles, respectively. The centrality dependence of the ratio, $R_{200/130}$, is shown in Fig. 11(b). The solid curves in the figure represent calculations within a gluon saturation model [49], while the dashed curves represent two-component fits to the data [58]. The gluon saturation model is able to reproduce the measured centrality and energy dependences reasonably well, though the particle multiplicity may not have strong discriminating power. Over a much broader energy range, the charged particle multiplicity is found to vary smoothly from AGS energies ($\sqrt{s_{\rm NN}} \approx$ few GeV) to the top RHIC energy ($\sqrt{s_{\rm NN}}$=200 GeV)[59] (see Fig. 26). This smooth energy dependence must be reconciled with any theoretical account invoking the crossing of a phase transition somewhere within this two-order-of-magnitude span. In particular, it is not obvious that the collisions should reach the gluon saturation regime over that entire span.

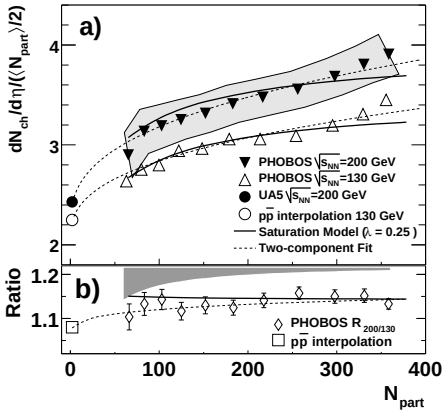

Fig. 11. (a) The measured pseudorapidity density $dN_{ch}/d\eta_{|\eta|\leq 1}/(1/2\langle N_{part}\rangle)$ as a function of N_{part} for Au+Au collisions at $\sqrt{s_{\rm NN}}$= 130 GeV (open triangles) and 200 GeV (closed triangles). The open and solid circles are $\overline{p}p$ collision results. (b) The ratio of charged multiplicity for $\sqrt{s_{\rm NN}}$= 130 GeV and 200 GeV. Saturation model calculations and two-component fits from [58] are shown as solid and dashed lines, respectively.

Figure 12 shows STAR measurements of integrated hadron yield ratios for central Au+Au collisions. These are used to constrain the values of system temperature and baryon chemical potential at chemical freeze-out, under the statistical model assumption that the system is in thermodynamic equilibrium at that stage. The excellent fit obtained to the ratios in frame (a) of the figure, including stable and long-lived hadrons through multi-strange baryons, is consistent with the light flavors, u, d, and s, having reached chemical equilibrium (for central collisions only) at $T_{ch} \approx 160 - 170$ MeV [26,60]. This temperature is close to the critical value for a QGP-to-hadron-gas transition predicted by LQCD [4,5], but is also close to the Hagedorn limit for a hadron resonance gas, predicted without any consideration of quark and gluon degrees of freedom [15]. Note that short-lived resonances show a deviation from the statistical model fits, as indicated by the K^*/K ratio in Fig. 12(b), suggesting that there is a fair amount of hadronic rescattering after the chemical

freeze-out.

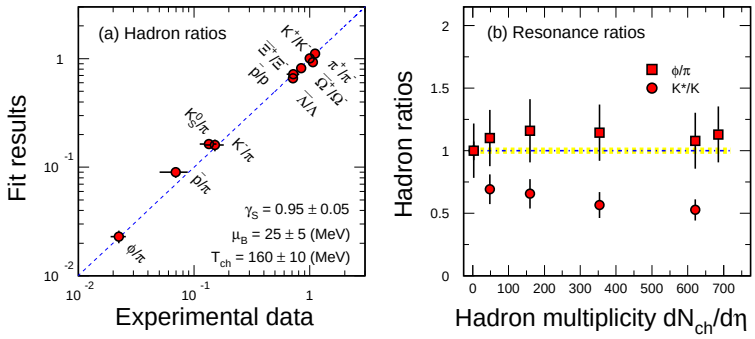

Fig. 12. (a) Hadron yield ratios measured in STAR for central Au+Au collisions. The x-and y-axes represent, respectively, the measured and chemical model fitted ratios. (b) Resonance ratios of ϕ/π (squares) and K^*/K (circles) versus the mid-rapidity charged multiplicity. The ratios from Au+Au collisions are normalized to the ratio from minimum bias $p+p$collisions. The error bars are quadratic sums of the statistical and systematic errors.

3.2 Hadron Spectra

In Fig. 13, the mid-rapidity transverse momentum distributions for pions, kaons, protons [67], ϕ [68], Ξ, and Ω [69], from $\sqrt{s_{\rm NN}}$= 200 GeV Au+Au collisions, are shown. The invariant spectra are plotted as a function of $m_T -$ mass $\equiv \sqrt{p_T^2 + \text{mass}^2} -$ mass. While the pion spectra show a power-law shape, most of the hadron spectra are exponential, especially for the hadrons containing strange valence quarks, such as K, ϕ, Ξ and Ω. In order to characterize the transverse motion, hydrodynamics-motivated fits [70] have been made to the measured spectra, permitting extraction of parameters representing the kinetic freeze-out temperature T_{fo} and collective radial velocity $\langle\beta_T\rangle$. The results are shown in Fig. 14.

Figure 14 shows that as the collisions become more and more central, the bulk of the system, dominated by the yields of π, K, p, appears to grow cooler at kinetic freeze-out and to develop stronger collective flow, suggesting a more rapid expansion after chemical freeze-out. For the most central collisions, the kinetic freeze-out temperature and velocity are $T_{fo} \sim 100$ MeV and $\beta_T \sim 0.6c$. On the other hand, for the same central collisions, the multi-strange particles ϕ and Ω freeze out at a higher temperature $T_{fo} \sim 180$ MeV, much closer to the point at which chemical freeze-out occurs [71]. Similar results have been seen as well in Au+Au collisions at $\sqrt{s_{\rm NN}}$= 130 GeV [72].

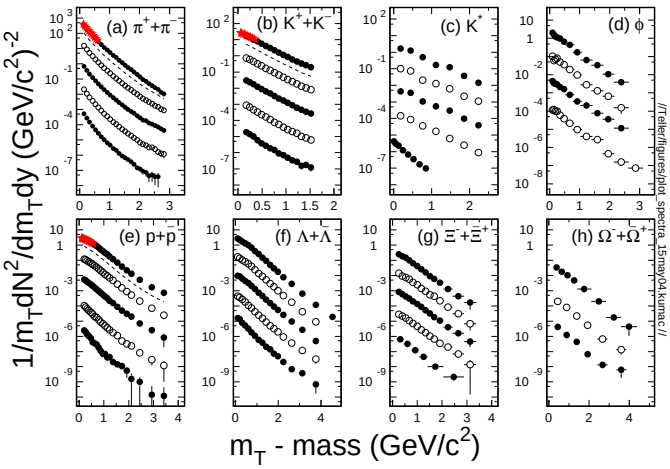

Fig. 13. Mid-rapidity hadron spectra from $\sqrt{s_{\rm NN}}$= 200 GeV Au+Au collisions. The spectra are displayed for steadily decreasing centrality from the top downwards within each frame, with dashed curves representing spectra from minimum-bias collisions. For pions (a), kaons (b), and protons (e) [67], the centrality bins are: 0-5%, 20-30% (scaled down by 10^{-1}), 40-50% (10^{-2}), 60-70% (10^{-3}), and 80-92% (10^{-4}). The star symbols (0-5%) are data from [60]. For K^* (c), from top to bottom, the centralities are 0-10%, 10-30%, 30-50%, 50-80% for Au+Au collisions and $p+p$collisions. For the ϕ-meson (d) [68], the centralities are: 0-5%, 10-30% (10^{-1}), 30-50% (10^{-2}), and 50-80% (10^{-3}). For Λ (f) and Ξ (g) [69], the centrality bins are: 0-5%, 10-20% (10^{-1}), 20-40% (10^{-2}), 40-60% (10^{-3}), 60-80% (10^{-4}). For the Ω baryon (h) [69], the centralities are: 0-10%, 20-40% (2×10^{-2}), and 40-60% (10^{-3}).

Since multi-strange hadrons have generally smaller hadronic cross sections [73] than particles with only u and d valence quarks, they decouple from the fireball early, perhaps right at the point of chemical freeze-out. That can account for the lower $\langle\beta_T\rangle$ and higher temperature values extracted from the spectrum fits for the multi-strange hadrons, see Fig. 14. Most importantly their finite value of $\langle\beta_T\rangle$ would then have to be accumulated prior to the chemical freeze-out, perhaps via partonic interactions during the earlier collision stages.

The ratio R_{CP} of hadron yields for central vs. peripheral bins are shown as a function of p_T in Fig. 15 (a) and (b), for mesons and baryons, respectively. For reference, the ratio for all charged hadrons is shown as the dot-dashed line in both plots. All the ratios are scaled by the expected ratio of contributing binary nucleon-nucleon collisions in the two centrality bins. The clear difference seen in the centrality dependence of baryons vs. mesons is one of the defining features of the intermediate p_T range from $\sim$ 1.5 to $\sim$ 6 GeV/c in RHIC heavy-ion collisions, and it cannot be understood from $p+p$ collision results. Another defining feature of this medium p_T range, to be discussed further below, is a similar meson-baryon difference in elliptic flow. Both facets of the meson-baryon differences can be explained naturally in quark recombination models for hadron formation [52].

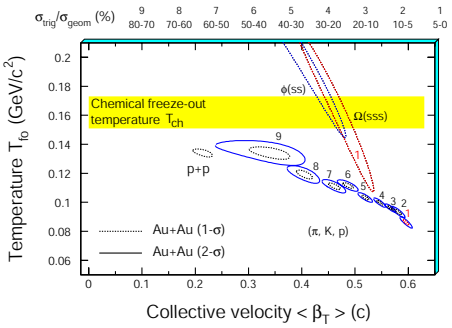

Fig. 14. The χ^2 contours, extracted from thermal + radial flow fits, for copiously produced hadrons π, K and p and multi-strange hadrons ϕ and Ω. On the top of the plot, the numerical labels indicate the centrality selection. For π, K and p, 9 centrality bins (from top 5% to 70-80%) were used for $\sqrt{s_{NN}} = 200$ GeV Au+Au collisions [60]. The results from $p+p$ collisions are also shown. For ϕ and Ω, only the most central results are presented. Dashed and solid lines are the 1-σ and 2-σ contours, respectively.

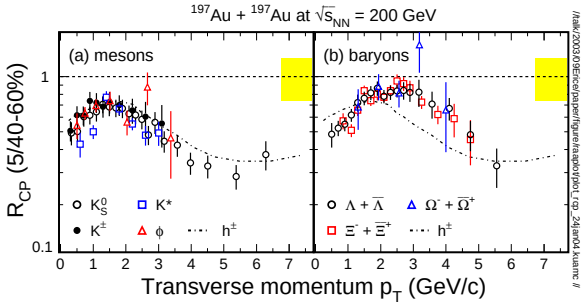

Fig. 15. STAR preliminary results for the ratio of mid-rapidity hadron yields R_{CP} in a central (0-5%) over a peripheral (40-60%) bin, plotted vs. p_T for mesons (a) and baryons (b). The yields are scaled in each centrality region by the calculated number N_{bin} of binary contributing nucleon-nucleon collisions. The width of the gray band around the line at unity represents the systematic uncertainty in model calculations of the centrality dependence of N_{bin}. R_{CP} for the sample of all charged hadrons is also shown by dot-dashed curves in both plots. The error bars on the measured ratios include both statistical and systematic uncertainties.

3.3 Hadron yields versus the reaction plane

In non-central heavy-ion collisions, the beam direction and the impact parameter define a reaction plane for each event, and hence a preferred azimuthal orientation. The orientation of this plane can be estimated experimentally by various methods, *e.g.*, using 2- or 4-particle correlations [74], with different sensitivities to azimuthal anisotropies not associated with collective flow. The observed particle yield versus azimuthal angle with respect to the event-by-event reaction plane promises information on the early collision dynam-

ics [57,61]. The anisotropy of the particle yield versus the reaction plane can be characterized in a Fourier expansion. Due to the geometry of the collision overlap region the second coefficient of this Fourier series – v_2, known as the elliptic flow for obvious reasons – is expected to be the dominant contribution.

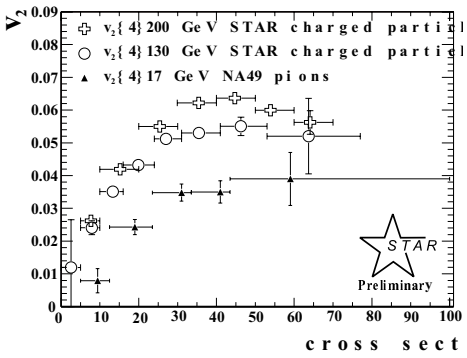

Fig. 16. Centrality dependence of v_2, integrated over p_T . The triangles are the NA49 measurements for pions at $\sqrt{s_{NN}} = 17$ GeV. The circles and crosses are STAR measurements for charged particles at $\sqrt{s_{NN}} = 130$ GeV and 200 GeV, respectively. The 4-particle cumulant method has been used to determine v_2 in each case. (Hydro pre/post-dictions still have to be included).

Figure 16 shows the mid-rapidity elliptic flow measurements, integrated over transverse momentum, as a function of collision centrality for one SPS and two RHIC energies. One clearly observes a characteristic centrality dependence that reflects the increase of the initial spatial eccentricity of the collision overlap geometry with increasing impact parameter. The integrated elliptic flow value for produced particles increases about 70% from the top SPS energy to the top RHIC energy, and it appears to do so smoothly as a function of energy (see Fig. 27).

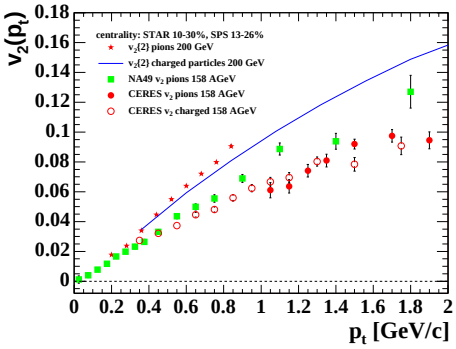

Fig. 17. $v_2(p_t)$ for one centrality (10-30%) range. The circles and squares are the CERES [75] and NA49 [76] measurements, respectively, at $\sqrt{s_{NN}} = 17$ GeV. The stars and the solid line are STAR measurements for pions and for all charged particles, respectively, at $\sqrt{s_{NN}} = 200$ GeV (evaluated here by the 2-particle correlation method). (Hydro pre/post-dictions still have to be included).

The origin of the energy dependence can be discerned by examining the differential $v_2(p_t)$, shown for the centrality selection 10–30% in Fig. 17. The com-

parison of the results for pions at $\sqrt{s_{NN}} = 200$ GeV and at the top SPS energy clearly reveals an increase in slope vs. p_T that accounts for approximately 50% of the increase in p_T -integrated v_2 from SPS to RHIC. The remaining half of the change is due to the increase in $\langle p_t \rangle$.

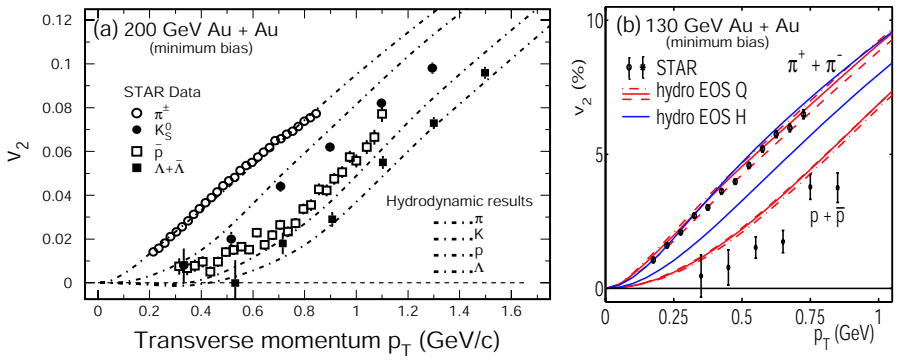

Fig. 18. (a) STAR experimental results of the transverse momentum dependence of the elliptic flow parameter in 200 GeV Au+Au collisions for charged $\pi^+ + \pi^-$, K^0_s , $\overline{p}$, and Λ [63]. Hydrodynamic calculations [20,64] assuming early thermalization, ideal fluid expansion, an equation of state consistent with LQCD calculations including a phase transition, and a sharp chemical freeze-out, are shown as dot-dashed lines. Only the lower p_T portion ($p_T \leq 1.5$ GeV/c) of the distributions is shown. (b) Hydrodynamics calculations of the same sort as in (a), now for a hadron vs. QGP EOS [11], compared to STAR v_2 measurements for minimum bias 130 GeV Au+Au collisions [77].

Collective motion leads to predictable behavior of the shape of the momentum spectra as a function of particle mass, as seen in the single inclusive spectra in Fig. 13. It is even more obvious in the dependence of $v_2(p_t)$ for the different mass particles. Figure 18 shows the measured low-p_T $v2$ distributions from 200 GeV Au+Au minimum bias collisions. Shown are the measurements for charged pions, K^0_S, antiprotons and Λ[63]. The clear, systematic mass-dependence of v_2 shown by the data is a strong indicator that a common transverse velocity field underlies the observations. This mass-dependence, as well as the absolute magnitude of v_2, is reproduced well by the hydrodynamics calculations shown in Fig. 18. Parameters of these calculations have been tuned to achieve good agreement with the measured spectra for different particles.

The agreement of these hydrodynamics calculations, which assume ideal relativistic fluid flow, with RHIC spectra and v_2 results is one of the most important results yet to emerge from RHIC! The agreement appears to be optimized when it is assumed that local thermal equilibrium is attained very early ($\tau < 1$ fm/c) during the collision, and that the hydrodynamic expansion passes through a stage characterized by a very soft EOS, consistent with the LQCD-predicted phase transition from QGP to hadron gas [17,20,11](see Fig. 18 (b)). The particular calculations in Fig. 18 [20,64] further invoke a simplified treat-

ment with a sharp onset of chemical freeze-out. With this assumption, they overpredict the elliptic flow for more peripheral RHIC collisions and for lower energies. However, alternative calculations combining hydrodynamics for the partonic stage with a hadron transport approach to the hadronic stage yield similar success in accounting for RHIC results, while also offering the promise of a reasonable account for the observed smooth energy dependence of p_T - integrated v_2 [17] (see Fig. 9). The currently unsettled question stimulated by the success of these hydrodynamics calculations is whether the simultaneous invocation of early thermalization and a soft mixed-phase EOS represents a unique solution to fitting the data. Might one do equally well by allowing thermal equilibrium to set in considerably later during the collision, but using a harder EOS, in which case the argument for QGP formation is considerably less compelling?

At higher p_T values, as shown by experimental results from 200 GeV Au+Au minimum bias collisions in Fig. 19, the observed values of v_2 saturate and the level of the saturation differs substantially between mesons and baryons. Hydrodynamics calculations overpredict the flow in this region. The dot-dashed curves in Fig. 19(a)-(c) represent simple analytical function fits to the measured K^0_S and $\Lambda + \bar{\Lambda}$ v_2 distributions [65]. It is then seen in Fig. 19 (b) and (c) that STAR's most recent v_2 results for the multi-strange baryons Ξ and Ω [66] are consistent with that of Λs within still sizable statistical uncertainties.

In Fig. 19 (d), all of STAR's particle-identified elliptic flow measurements for the 200 GeV Au+Au minimum-bias sample are combined by dividing both v_2 and p_T by the number of constituent quarks (n_q) in the hadron of interest. The apparent scaling behavior seen in this figure is very significant, as the data themselves seem to be pointing to constituent quarks as the most effective degree of freedom in determining hadron flow at intermediate p_T values! The scaling appears to work surprisingly well even at low p_T, except for the pions, which may often result from the decay of heavier hadrons. On the other hand, the data in Fig. 18 make an even more compelling case that the v_2 results at low p_T exhibit a clear mass-dependence expected from hydrodynamics, and in this light the success of constituent quark scaling for low p_T in Fig. 19 (d) appears somewhat accidental. However, if the scaling behavior at intermediate p_T is confirmed with improved data, and extended to more hadron species, this gives a profound clue to the origin of the meson-baryon differences (see also Fig. 15) that characterize this p_T range. In particular, both the v_2 scaling and the meson-baryon R_{CP} differences can be explained by assuming that hadron formation at moderate p_T proceeds predominantly via the coalescence of n_q constituent quarks at transverse momenta $\sim p_T/n_q$, drawn from a thermal (exponential) spectrum [52]. These constituent quarks would have to carry their own substantial azimuthal anisotropy – summed to give the hadron v_2 – which might arise from collective partonic flow at a collision stage preceding the hadronization.

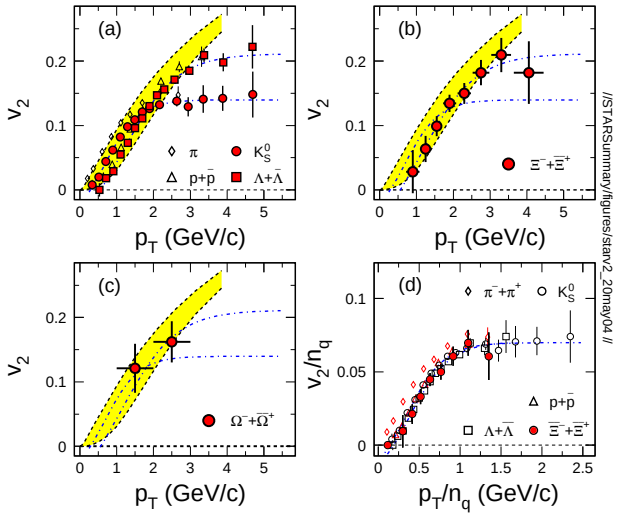

Fig. 19. (a) STAR experimental results of the transverse momentum dependence of the event elliptic anisotropy parameter for π, K^0_S, $p+\overline{p}$, $\Lambda+\overline{\Lambda}$, all produced in minimum-bias Au+Au collisions at $\sqrt{s_{NN}} = 200$ GeV. Dot-dashed lines are fits to the data using simple analytic functions. Hydrodynamic calculations are indicated by the shaded bands. Multi-strange baryon elliptic flow is shown in (b) for Ξ and (c) for Ω. (d) Flow results for all of the above hadrons (except the statistically limited Ω) combined by scaling both v_2 and p_T by the number of constituent quarks (n_q) in each hadron.

In summary, the measured yields with respect to the reaction plane provide critical hints of the properties of the collision matter at early stages. They indicate that it behaves collectively, and is consistent with rapid (*i.e.*, very short mean free path) attainment of local thermal equilibrium in a QGP phase. Hydrodynamic accounts for the mass- and p_T-dependence of v_2 for soft hadrons appear to favor system evolution through a soft, mixed-phase EOS. The saturated v_2 values observed for identified mesons and baryons in the range $2 \lesssim p_T \lesssim 6$ GeV/c suggest that hadronization in this region occurs via coalescence of collectively flowing constituent quarks. What has yet to be demonstrated is that these interpretations are unique and robust against improvements to both the measurements and the theory.

3.4 Correlation Analyses

Two-hadron correlation measurements in principle should provide valuable information on the phase structure of the system at freeze-out. From the experimentally measured momentum-space two-particle correlation functions, a Fourier transformation is then performed in order to extract information on the space-time structure [80]. Bertsch-Pratt parameterization [81] is often used to decompose total momentum in such measurements into components parallel

to the beam (*long*), parallel to the pair transverse component (*out*) and along the remaining third direction (*side*). In this Cartesian system, information on the source duration time is mixed into the *out* components. Hence, the ratio of inferred emitting source radii R_{out}/R_{side} is sensitive to the time duration of the source emission. For example, if a QGP is formed in collisions at RHIC, a long duration time and consequently large value of R_{out}/R_{side} are anticipated [82].

Measurement results for Hanbury-Brown-Twiss (HBT) pion interferometry, exploiting the boson symmetry of the two detected particles at low relative momenta, are shown in Figs. 20 and 21. A clear dependence of the 'size' parameters on the pair transverse momentum k_t is characteristic of collective expansion of the source [78,79], so the results are plotted vs. k_t in Fig. 20. As indicated by the set of curves in the figure, hydrodynamics calculations that can account for hadron spectra and elliptic flow at RHIC systematically overpredict R_{out}/R_{side} [78,83]. The implication that the collective expansion does not last as long in reality as in the hydrodynamics accounts is reinforced by systematic study of HBT correlations relative to the event-by-event reaction plane [79]. The source eccentricity at freeze-out inferred from these measurements is shown in Fig. 21 to retain a significant fraction of the initial spatial eccentricity characteristic of the impact parameter for each centrality bin. It thus appears that the pressure and expansion time of the collision system are not sufficient to completely quench its initial configuration-space anisotropy, in contrast to hydrodynamics expectations (see Fig. 6).

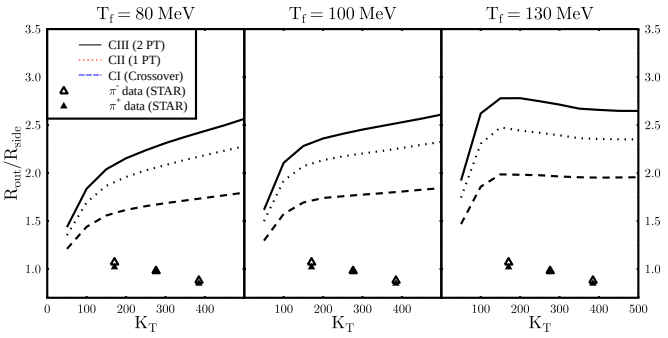

Fig. 20. STAR measurements [78] of R_{out}/R_{side} from pion HBT correlations for central Au+Au collisions, plotted as a function of the pion pair transverse momentum k_t. The experimental results are identical in the three frames, but are compared to hydrodynamics calculations [83] performed for a variety of parameter values.

The failure of the hydrodynamics calculations to account for the HBT results poses a serious question regarding the robustness of the hydrodynamics success in reproducing v_2 and radial flow data. Although the HBT interference only emerges after the freeze-out of the strong interaction, whose treatment is beyond the scope of hydrodynamics, the measured correlation functions encode information from the entire system space-time evolution toward the emitting

source shape [84]. Furthermore, these HBT results are extracted from the low p_T region, where soft bulk production dominates. It is thus reasonable to expect the correct hydrodynamics account of the collective expansion to be consistent with the HBT data. If improved treatment of the hadronic stage is necessary to attain this consistency, then it is important to see how those improvements affect the agreement with elliptic flow and spectra.

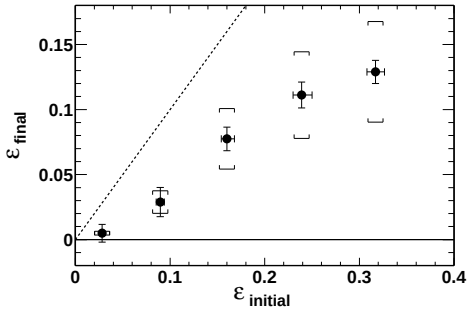

Fig. 21. The eccentricity ϵ_{final} of the emitting source of soft pions, inferred from STAR HBT correlations measured with respect to the reaction plane, plotted versus the initial spatial eccentricity $\epsilon_{initial}$ deduced from a Glauber calculation for six different Au+Au centrality bins. See [79] for details.

Angular correlations of pairs of hadrons can cast additional light on the nature of the interactions that lead to collective behavior of the matter formed in RHIC collisions, and on the mechanisms of hadron production. Since most RHIC measurements of pairwise angular correlations have so far been undertaken to explore the quenching of jets in the produced matter, these results will be described in the following chapter.

3.5 Fluctuation analyses

A system evolving near a phase boundary should develop significant dynamical fluctuations away from the mean thermodynamic properties of the matter. For high-energy heavy ion collisions, it has been predicted that the study of fluctuations might provide evidence for the formation of matter with partonic degrees of freedom [85–90]. In addition, nonstatistical fluctuations could also be introduced by incomplete equilibrium [91]. With its large acceptance and complete event-by-event reconstruction capabilities, the STAR detector holds great potential for fluctuation analyses of RHIC collisions.

Relevant analysis efforts to date have focused on the balance function [92], characterizing pseudorapidity difference distributions between oppositely charged hadrons, and on event-to-event fluctuations in mean p_T value [95] and in charged hadron multiplicity [94]. The balance function widths have been observed to decrease smoothly with increasing charged hadron multiplicity for

both $\sqrt{s_{\rm NN}}$= 130 GeV and 200 GeV, and in $p+p$, d+Au , and Au+Au collisions [92,96]. This observation is consistent with the trend predicted by models incorporating delayed hadronization [89]. The narrow width of the measured balance function can also be reproduced by the quark recombination approach [93]. As a function of collision centrality, a smooth variation of the $\langle p_T \rangle$ fluctuation amplitude has also been observed [95,96], with evidence of non-statistical fluctuations reported for the 15% most central 130 GeV Au+Au collisions [95]. The charged hadron multiplicity analysis appears to indicate fluctuations at a level that might be expected if the system behaved like a resonance gas [94].

It has been difficult to date to extract clear lessons regarding the nature of the bulk collision matter from these fluctuation analyses, for two reasons: the analysis methods, both in theory and in their application to the finite systems created in high energy collisions and characterized in non-hermetic detectors, are still in their infancy; non-statistical fluctuations in any one parameter, once identified, can still arise from a variety of sources. Nonetheless, if a systematic body of dynamical fluctuation results can be established, they continue to hold the promise to illuminate the collision system in ways we are not otherwise clever enough to probe more directly.

3.6 Summary and Open Questions

In this chapter, we have presented important RHIC results on the bulk properties attained in Au+Au collisions at RHIC. The measured hadron spectra, yield ratios, and low p_T v_2, are all consistent from all experiments at RHIC, and they clearly reveal a collective velocity field in such collisions. When interpreted within the context of statistical and hydrodynamical models, they strongly suggest that at least approximate local thermal equilibrium is reached early, and spanning the u, d and s sectors, in the most central collisions. The radial and elliptic flow results for multi-strange hadrons, and for mesons vs. baryons at moderate p_T values, hint that the collectivity is developed prior to hadronization, in a manner consistent with constituent quark coalescence approaches. However, the pion interferometry results cast doubt on the hydrodynamics interpretation.

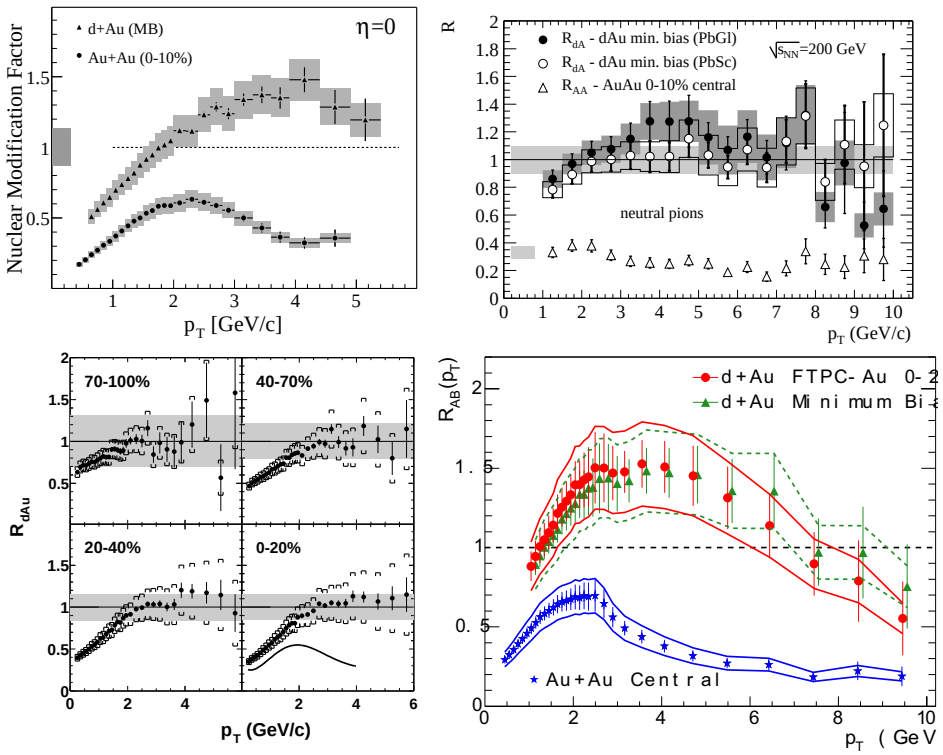

Fig. 22. Binary-scaled ratio $R_{AB}(p_T)$ (Eq. 4) of charged hadron and π^0 inclusive yields from 200 GeV Au+Au and d+Au relative to that from p+p collisions, from BRAHMS[97] (upper left), PHENIX[98] (upper right), PHOBOS[99] (lower left) and STAR[100] (lower right). The PHOBOS data points in the lower left frame are for d+Au only. The shaded horizontal bands around unity represent the systematic uncertainties in the binary scaling corrections.

4 Hard Probes

Due to the transient nature of the matter created in high energy nuclear collisions, external probes cannot be used to study its properties. However, the dynamical processes that produce the bulk medium also produce energetic particles through hard scattering processes. The interaction of these energetic particles with the medium provides a class of unique, penetrating probes that are analogous to the method of computed tomography (CT) in medical science

4.1 Inclusive hadron yields at high p_T

There are several results to date from RHIC pertaining to this approach and the magnitude of the observed effects is large. Figures 22 and 23 show the most significant high p_T measurements made at RHIC thus far. Both figures incorporate measurements of $\sqrt{s_{\rm NN}}$=200 GeV p+p, d+Au and centrality-selected Au+Au collisions at RHIC, with the simpler p+p and d+Au systems providing

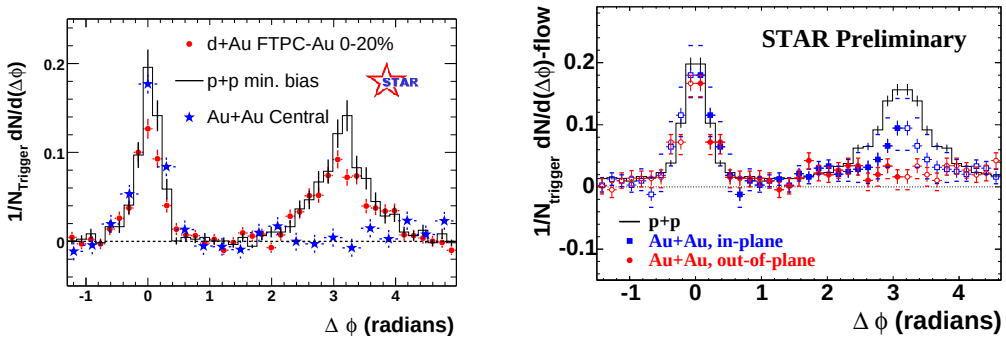

Fig. 23. Dihadron azimuthal correlations at high p_T. Left panel shows correlations for p+p, central d+Au and central Au+Au collisions (background subtracted) from STAR [100,101]. Right panel shows the background-subtracted high p_T dihadron correlation for different orientations of the trigger hadron relative to the reaction plane [102,103].

benchmarks for phenomena seen in the more complex Au+Au collisions.

Figure 22 shows $R_{AB}(p_T)$, the ratio of inclusive charged hadron yields in A+B (either Au+Au or d+Au) collisions to p+p, corrected for trivial geometric effects via scaling by $\langle N_{bin} \rangle$ the calculated mean number of binary nucleon-nucleon collisions contributing to each A+B centrality bin:

$$R_{AB}(p_T) = \frac{d\sigma_{AB}/dyd^2p_T}{\langle N_{bin} \rangle d\sigma_{NN}/dyd^2p_T}. \quad (4)$$

A striking phenomenon is seen: large p_T hadrons in central Au+Au collisions are suppressed by a factor ≈ 5 relative to naive (binary scaling) expectations. Conventional nuclear effects, such as nuclear shadowing of the parton distribution functions and initial state multiple scattering, cannot account for the suppression. Furthermore, the suppression is not seen in d+Au but is unique to Au+Au collisions, proving experimentally that it results not from nuclear effects in the initial state (in particular, gluon saturation), but rather from the final state interaction of hard scattered partons or their fragmentation products in the dense medium generated in Au+Au collisions [97–100].

4.2 Dihadron azimuthal correlations

Figure 23 shows correlations of high p_T hadrons. The left panel shows the azimuthal distribution of hadrons with p_T>2 GeV/c relative to a trigger hadron with $p_T{}^{\rm trig}$>4 GeV/c. A hadron pair drawn from a single jet will generate an enhanced correlation at $\Delta\phi \sim 0$, as observed for p+p, d+Au and Au+Au, with similar correlation strengths and widths. A hadron pair drawn from back-to-back dijets will generate an enhanced correlation at $\Delta\phi \sim \pi$, as observed

for p+p and for d+Au with somewhat broader width than the near-side correlation peak. However, the back-to-back dihadron correlation is strikingly, and uniquely, absent in central Au+Au collisions. If the correlation is indeed the result of jet fragmentation, the suppression is again due to the final state interaction of hard scattered partons or their fragmentation products in the dense medium generated in Au+Au collisions [100]. In this environment, the hard hadrons we do see (and hence, the near-side correlation peak) would arise preferentially from partons scattered outward from the surface region of the collision zone, while the away-side partons must burrow through significant lengths of dense matter.

The qualification concerning the dominance of jet fragmentation is needed in this case, because the correlations have been measured to date primarily for hadrons in that intermediate p_T range (2-6 GeV/c) where sizable differences in meson vs. baryon yields have been observed (see Fig. 15), in contrast to expectations for jets fragmenting in vacuum. The systematics of the meson-baryon differences in this region suggest sizable contributions from softer mechanisms, such as quark coalescence [52]. Where the azimuthal correlation measurements have been extended to trigger particles above 6 GeV/c, they show a similar pattern to the results in Fig. 23, but with larger statistical uncertainties [104]. This suggests that the peak structures in the correlations do, indeed, reflect dijet production, and that the back-to-back suppression is indeed due to jet quenching. Coalescence processes in the intermediate p_T range may contribute predominantly to the smooth background, with only elliptic flow correlations, that has already been subtracted from the data in Fig. 23.

A more differential probe of partonic energy loss is the measurement of high p_T dihadron correlations relative to the reaction plane orientation. The right panel of Fig. 23 shows a preliminary study from STAR of the high p_T dihadron correlation from 20-60% centrality Au+Au collisions, with the trigger hadron situated in the azimuthal quadrants centered either in the reaction plane ("in-plane") or orthogonal to it ("out-of-plane") [102,103]. The same-side dihadron correlation in both cases is similar to that in p+p collisions. In contrast, the suppression of the back-to-back correlation depends strongly on the relative angle between the trigger hadron and the reaction plane. This systematic dependence is consistent with the picture of partonic energy loss: the path length in medium for a dijet oriented out of the reaction plane is longer than in the reaction plane, leading to correspondingly larger energy loss. The dependence of parton energy loss on path length is predicted [34] to be substantially stronger than linear.

The energy lost by away-side partons traversing the collision matter must appear, in order to conserve transverse momentum, in the form of an excess of softer emerging hadrons. An analysis of azimuthal correlations between hard and *soft* hadrons has thus been carried out for both 200 GeV p+p and Au+Au

collisions [105] in STAR, as a first attempt to trace the degree of degradation on the away side. With trigger hadrons still in the range 4< p_T^{trig} <6 GeV/c, but the associated hadrons now sought over 0.15< p_T <4 GeV/c, combinatorial coincidences dominate these correlations, and they must be removed statistically by a careful mixed-event subtraction, with an elliptic flow correlation correction added by hand [105]. The results demonstrate that, in comparison with p+p and peripheral Au+Au collisions, the momentum-balancing hadrons opposite a high-p_T trigger in central Au+Au are greater in number, much more widely dispersed in azimuthal angle, and significantly softer. The latter point is illustrated in Fig. 24, showing the centrality dependence of <p_T>of the associated away-side charged hadrons in comparison to that of the bulk inclusive hadrons. While in peripheral collisions the values of <p_T>for the away-side hadrons are significantly larger than that of inclusive hadrons, the two values approach each other with increasing centrality. These results are again subject to the ambiguity arising from possible soft (*e.g.*, coalescence) contributions to the observed correlations, as the away-side strength shows little remnant of jet-like behavior [105]. They will be extended to higher trigger-hadron p_T values. If a hard-scattering interpretation framework turns out to be valid, the results suggest that even a moderately hard parton traversing a significant path length through the collision matter makes substantial progress toward equilibration with the bulk. The rapid attainment of thermalization via the multitude of softer parton-parton interactions in the earliest collision stages would then not be surprising.

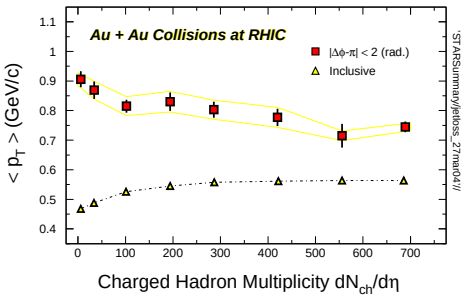

Fig. 24. Associated charged hadron <p_T>from the away-side in 200 GeV p+p (leftmost point) and Au+Au collisions (squares). The band represents the systematic uncertainties in Au+Au collisions. Inclusive results are shown as triangles.

4.3 Theoretical interpretation of hadron suppression

Figure 25 shows $R_{CP}(p_T)$, the binary scaled ratio of yields from central relative to peripheral collisions for charged hadrons from 200 GeV Au+Au interactions. $R_{CP}(p_T)$ is closely related to $R_{AB}(p_T)$, using as reference the binary-scaled spectrum from peripheral Au+Au collisions rather than p+p collisions.

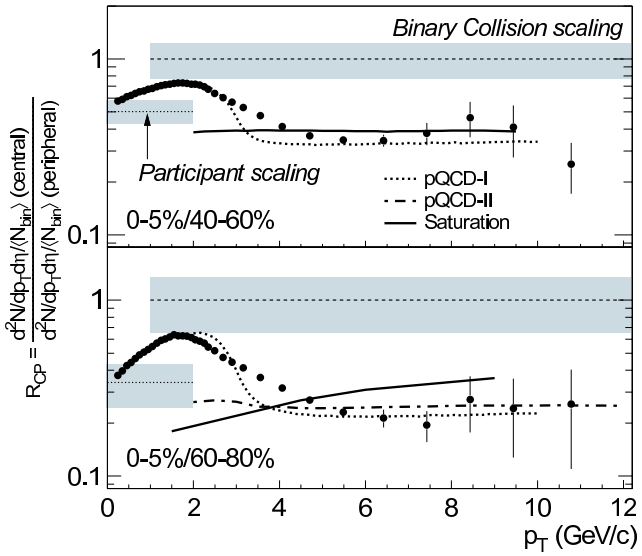

Fig. 25. Binary-scaled yield ratio $R_{CP}(p_T)$ for central (0-5%) relative to peripheral (40-60%, 60-80%) collisions for charged hadrons from 200 GeV Au+Au collisions [109]. The shaded bands show the multiplicative uncertainty of the normalization of $R_{CP}(p_T)$ relative to binary collision and participant number scaling.

The substitution of the reference set allows a slight extension in the p_T range for which useful ratios can be extracted. The error bars at the highest p_T are dominated by statistics and are therefore, to a large extent, uncorrelated between the two centrality bins. The suppression for central is again seen to be a factor ≈ 5 relative to the most peripheral collisions, and for $p_T > \sim 6$ GeV/c it is independent of p_T within experimental uncertainties. Also shown in Fig. 25 are results from theoretical calculations based on pQCD incorporating partonic energy loss in dense matter (pQCD-I [106], pQCD-II [107]) and on suppression at high p_T due to gluon saturation effects (Saturation [108]). The negligible p_T-dependence of the suppression at high p_T is a prediction of the pQCD models [106,107], resulting from the subtle interplay of partonic energy loss, Cronin (initial-state multiple scattering) enhancement, and nuclear shadowing. The variation in the suppression for $p_T \lesssim 5$ GeV/c is related to differences in suppression in this region for mesons and baryons (see Fig. 15). It is accounted for in the pQCD-I calculation by the introduction of an additional non-fragmentation production mechanism for kaons and protons. The magnitude of the hadron suppression in the pQCD calculations is adjusted to fit the measurements for central collisions, as discussed further below.

It was proposed recently that gluon saturation effects can extend well beyond the saturation momentum scale Q_s, resulting in hadron suppression relative to binary scaling ($R_{AB}(p_T)<1$) for hadron $p_T \sim 5-10$ GeV/c at RHIC energies [108], in reasonable agreement with the data in Fig. 25. However, since this suppression originates in the properties of the incoming nuclear wave function, hadron production in d+Au collisions should also be suppressed by

this mechanism [108]. Experimentally, an enhancement in mid-rapidity hadron production in d+Au is seen instead (Figure 22 [98,100,99,97]), even in central d+Au collisions [100] where saturation effects should be most pronounced. The observed enhancement is at variance with saturation model expectations at high p_T [108]. More generally, the d+Au data clearly demonstrate that the strong hadron suppression seen in central Au+Au collisions at high p_T results from interaction of hard scattered partons or their fragmentation products in the dense medium generated in the collision.

In order to deduce the magnitude of *partonic* energy loss in the medium it is essential to establish the degree to which *hadronic* interactions, specifically the interaction of hadronic jet fragments with the medium, can at least in part generate the observed high p_T phenomena and contribute substantially to the jet quenching [110–112]. Simple considerations already argue against this scenario. The formation time of hadrons with energy E_h and mass m_h is $t_f = (E_h/m_h)\tau_f$, where the rest frame formation time $\tau_f \sim 0.5{-}0.8$ fm/c. Thus, a 10 GeV/c pion has formation time ~ 50 fm/c and is unlikely to interact as a fully formed pion in the medium. Since the formation time depends on the boost, the suppression due to hadronic absorption with constant or slowly varying cross section should turn off with rising p_T, at variance with observations (Fig. 25). A detailed hadronic transport calculation [112] leads to a similar conclusion: the absorption of formed hadrons in the medium cannot fails by a large factor to account for the observed suppression. Rather, this calculation attributes the suppression to *ad hoc* medium interactions of "pre-hadrons" with short formation time and constant cross section. The properties of these "pre-hadrons" are thus similar to those of colored partons [112], and not to the expected color transparency of hadronic matter to small color singlet particles that might evolve into normal hadrons [38].

Additional considerations of the available high p_T data [39] also support the conclusion that jet quenching in heavy ion collisions at RHIC is the consequence of partonic energy loss. In particular, large v_2 values observed at high p_T and the systematics of the small-angle dihadron correlations are difficult to reconcile with the hadronic absorption scenario. While further theoretical investigation of this question is certainly warranted, we conclude that there is no support in the data for *hadronic* absorption as the dominant mechanism underlying the observed suppression phenomena at high p_T and we consider *partonic* energy loss to be well established as its primary origin. It is conceivable that there may be minor hadronic contributions from the fragments of soft gluons radiated by the primary hard partons during their traversal of the collision matter.

The magnitude of the suppression at high p_T in central collisions is fit to the data in the pQCD-based models with partonic energy loss, by adjusting the initial gluon density of the medium. The agreement of the calculations with

the measurements at p_T>5 GeV/c is seen in Fig. 25 to be good. In order to describe the observed suppression, these models require an initial gluon density about a factor 50 greater than that of cold nuclear matter [106,107]. This is the main physics result of the high p_T studies carried out at RHIC to date. It should be kept in mind that the actual energy loss inferred for the rapidly expanding Au+Au collision matter is not very much larger than that inferred for static, cold nuclear matter from semi-inclusive deep inelastic scattering data [43]. But in order to account for this slightly larger energy loss *despite* the rapid expansion, one infers the much larger *initial* gluon density at the start of the expansion [106,107]. Certainly, then, the quantitative extraction of gluon density is subject to uncertainties from the theoretical treatment of the expansion and of the energy loss of partons in the entrance-channel cold nuclear matter before they initially collide.

The gluon density derived from energy loss calculations is consistent with estimates from the measured rapidity density of charged hadrons [113] using the Bjorken scenario [114], assuming isentropic expansion and duality between the number of initial gluons and final charged hadrons. Similar values are also deduced under the assumption that the initial state properties in central Au+Au RHIC collisions, and hence the measured particle multiplicities, are determined by gluon-gluon interactions below the gluon density saturation scale in the initial-state nuclei [49]. Additionally, the energy density can be estimated from global measurements. Given the measured total transverse energy $dE_T/d\eta \approx 540$ GeV, or about 0.8 GeV per charged hadron in central $Au+Au$ collisions at $\sqrt{s} = 130$ GeV [115], the initial energy density appears to be of order 50-100 times that in cold nuclear matter. These inferred densities fall well into the regime where LQCD calculations predict equilibrated matter to reside in the QGP phase.

4.4 Outlook

While large effects have been observed and the phenomenon of jet quenching in dense matter has been firmly established, precision data in a larger p_T range are needed to fully explore the jet quenching phenomena and their connection to properties of the dense matter. The region 2<p_T<6 GeV/c has significant contributions from non-perturbative processes other than vacuum fragmentation of partons, perhaps revealing novel hadronization mechanisms. All studies to date of azimuthal anisotropies and correlations of "jets" have by necessity been constrained to this region, with only the inclusive spectra extending to the range where hard scattering is expected to dominate the inclusive yield. High statistics data sets for much higher p_T hadrons are needed to fully exploit azimuthal asymmetries and correlations as measurements of partonic energy loss. Dihadron measurements probing the details of the fragmentation process

may be sensitive to the *energy* density, in addition to the gluon density that is probed with the present measurements. Heavy quark suppression is theoretically well controlled, and measurement of it will provide a critical check on the understanding of partonic energy loss. The *differential* measurement of energy loss through measurement of the emerging away-side jet and the recovery of the energy radiated in soft hadrons is still in its initial phase of study. A complete mapping of the modified fragmentation with larger initial jet energy and with a direct photon trigger will cross check the energy dependence of energy loss extracted from single inclusive hadron suppression. Experiments at different colliding energies are also essential to reveal the onset of critical phenomena, or at the minimum to map the variation of jet quenching with initial energy density and the lifetime of the dense system.

5 Some Open Issues

While evidence exists in support of a claim of the creation of a new state of matter in heavy ion collisions at RHIC, we must address how compelling this claim is. In this assessment, it is important to exercise the same degree of skepticism with which we might view a different scientific community (say in solid state physics or in chemistry) who claimed to make a new type of matter, different than anything else created on Earth. In this section, we briefly discuss open questions that should cause some hesitation before we, as a community, declare victory on the QGP.

5.1 Are crosschecks necessary? Are they possible?

Theoretical arguments that a confined state is impossible at energy densities apparently achieved at RHIC appear well-founded. Some experimental observations are consistent with the the creation of deconfined matter. However, the claim for creation of a fundamentally new state of matter becomes much more convincing when accompanied by experimental demonstration that the matter behaves qualitatively *differently* than "normal" matter (in our case, confined hadronic matter). Ideally, one would like to see cross-checks, in which a system we know/believe to be in a confined state does *not* exhibit behavior observed at RHIC.

Here we briefly discuss some of the key observations that underlie the claim of deconfined matter at RHIC, and ask whether cross-checks are necessary to support such a claim, or whether they are even possible.

5.1.1 Hard sector: Jet quenching

Inclusive spectra and two-particle azimuthal correlation measurements clearly demonstrate that jets are suppressed at RHIC, relative to scaled NN collisions. This suppression is usually viewed as arising from energy loss, in a deconfined medium, of the hard-scattered parton prior to fragmentation.

If the jet quenching is to be taken as an indication of deconfined matter, one would like to observe the *lack* of quenching when the medium is not in a deconfined state. Certainly, the lack of suppression (indeed, the enhancement, due to Cronin effect) in d+Au collisions at RHIC provides a critical cross-check that the suppression is not an initial-state effect.

However, might jets, for some reason other than QGP formation, *always* be suppressed in central A-A collisions? High-p_T yields from Pb-Pb collisions at

the SPS show an enhancement over a scaled *parameterized* p-p reference spectrum. However, initial-state ("Cronin") enhancement has not been measured at these energies, and the p-p parameterization has recently been called into question [119]. Also, it is unclear whether the suppression of away-side two-particle correlations out of the reaction plane, observed at RHIC are of similar origin as the away-side out-of-plane broadening observed at the SPS [116].

Thus it may be that jets in central A-A collisions at the SPS are suppressed. As at RHIC, this may be caused by QGP formation at the SPS. If this is assumed, an important cross-check would be to examine jet yields at even *lower* energies, at which QGP is not formed. However, even in p-p collisions, high-p_T yields drop precipitously at lower energies. So, by the time $\sqrt{s_{NN}}$ drops sufficiently that QGP is not formed, the jet yield may be negligible. Thus, we may ask:

Are high-p_T yields in central A-A collisions *always* suppressed relative to scaled p-A spectra? If so, is it because whenever $\sqrt{s_{NN}}$ is sufficiently high to produce jets, one is past the QGP threshold?

If so, then, unfortunately, a critical and compelling cross-check of a QGP signature appears impossible.

5.1.2 Firm sector: constituent-quark scaling of yields and anisotropies

The baryon/meson systematics of R_{AA} and constituent-quark-scaled elliptic flow represent some of the most compelling, data-based evidence of collective behavior of a system whose degrees of freedom are (constituent) quarks. The fact that such a simple picture is remarkably consistent with apparently "all" existing RHIC data in the intermediate p_T sector (ample– and plausible–excuses exist for the deviation of the pions from the systematic) is simply striking.

Once again, one would like to observe the *absence* of this behavior for systems in which QGP is not formed. High-quality, particle-identified elliptic flow data do not exist at SPS (or lower) energies in this p_T region.

Should constituent-quark scaling of v_2 in the intermediate p_T sector be broken if a QGP is *not* formed? If so, is a statistically meaningful, particle-identified measurement of v_2 at intermediate p_T possible at $\sqrt{s_{NN}}$ below the QGP threshold?

If not, then, again unfortunately, another critical and compelling cross-check of this QGP signature appears impossible.

5.1.3 Soft sector: strong elliptic flow in agreement with hydrodynamics

While the hard and firm sectors may not have been fully accessible at lower energies, thus not allowing important tests of the "newness" of signals at RHIC, the soft (low-p_T) sector has been extensively explored, even from Bevalac energies. Essentially the *only* observable selected as a "pillar" of the QGP claim at RHIC is the strong elliptic flow, which is in agreement with hydrodynamic models.

Hydrodynamics spectacularly reproduces the soft-sector momentum-space signatures of collective behavior at RHIC (radial and elliptic flow, as a function of p_T and mass). Further, the agreement is better with an Equation of State which includes a phase transition from hadronic to partonic matter.

The claim is often made that the strength of the elliptic flow has finally at RHIC energies reached the hydro "limit," suggesting creation of equilibrated matter at an early stage in the collision (when geometric anisotropy is still large). However, the experimental results clearly indicate a smoothly rising $v_2(\sqrt{s_{NN}})$, while the hydrodynamic limit for given initial spatial eccentricity is falling with increasing energy. Doesn't this combination suggest a coincidence of observation and prediction at *some* energy, regardless of the validity of the theory? Looking at the previously established elliptic flow excitation function, $(v_2(\sqrt{s_{NN}})$, one might ask why one would expect any flow strength *other* than that now observed at RHIC?

The case for hydrodynamics– and in particular for an Equation of State containing a phase change– would be much strengthened if, at higher $\sqrt{s_{NN}}$, the data do not surpass the "hydrodynamic limit," and at lower $\sqrt{s_{NN}}$, the predicted non-trivial energy dependence (dip in Fig. 7) were to be observed.

One of these important cross-checks (v_2 at higher $\sqrt{s_{NN}}$) will need to wait until LHC turns on. The other is potentially possible at RHIC with an energy scan program (already underway).

Should we expect to observe non-trivial structure in the excitation function of v_2 at lower RHIC energies, as predicted by hydrodynamics, or is thermalization insufficiently established below $\sqrt{s_{NN}} \approx 100$ GeV for hydro to be valid?

Perhaps thermalization in non-central Au+Au collisions at lower energies is insufficient to perform this important cross-check with those systems. It has been suggested that U+U collisions, triggered on the geometric situation of zero impact parameter and full alignment of the transversely-directed major

axes of the deformed shape, may yet allow these tests to be performed.

It will be unfortunate if, due to incomplete thermalization, the low-energy cross-check is impossible, while achievable collision energies do not allow the high-energy cross-check for another five years.

5.1.4 What if all cross-checks are impossible?

The three observations mentioned above feature among the "heretofore unobserved phenomena" seen at RHIC, and are taken as evidence of QGP formation. A skeptic (or cynic) familiar with the history of our field, however, might suggest that a *truly* new occurrence would be a theoretical framework which, having experienced success at one energy, quantitatively survives systematic cross-checks. In this regard, excitation functions have played a crucial role in heavy ion physics.

For reasons mentioned above, lower-energy cross-checks, which would make the case much more compelling, might be impossible to perform. In this case, our reliance on theory is significantly increased, and the questions raised in the following subsections become important.

5.2 Do the observed consistencies with QGP formation demand a QGP-based explanation?

As mentioned above, much of the evidence for a new state of matter involves (an evolving) theoretical understanding; an experimentalist from another field, looking at the smooth trends in the data alone, would not immediately conclude "new" physics is at play.

As also mentioned above, the field of heavy ion physics is littered with models which work very well under certain conditions (usually at a given $\sqrt{s_{NN}}$), but whose assumptions are later shown invalid under cross-checks.

Here, we question the *uniqueness* of a QGP-based explanation. In other words, do the data *demand* a scenario characterized by deconfined matter?

5.2.1 Strong elliptic flow

RHIC v_2 results appear to follow smooth trends established by lower-energy heavy ion collisions, but not predicted by hydrodynamics. The hydrodynamic overestimate of elliptic flow at lower energies has generally been attributed to a failure to achieve complete thermalization. This interpretation suggests

that the energy-dependence of flow (as well as other) observations is dominated by the poorly understood dynamics of early thermalization, so that the apparent success at RHIC energies should be interpreted cautiously before one sees comparable success at other energies or initial deformations as well. While application of hydrodynamics relies on local thermal equilibrium, it is not obvious that agreement with data after parameter adjustment necessarily proves thermalization.

The unprecedented success of hydrodynamics calculations assuming ideal relativistic fluid behavior in accounting for RHIC elliptic flow results has been interpreted as evidence for both early attainment of local thermal equilibrium and a soft equation of state, characteristic of the predicted phase transition. How do we know that the observed elliptic flow can't result, alternatively, from a harder EOS coupled with incomplete thermalization?

Even if we *assume* thermalization (and hence the applicability of hydrodynamics), it is not immediately obvious that a complete evaluation of the "theoretical errorbars" has been performed.

When parameters are adjusted to reproduce spectra, agreement with v2 measurements in different centrality bins is typically at the 20-30% level. The continuing systematic discrepancies from HBT results and from the energy dependence of elliptic flow suggest some level of additional ambiguity from the freezeout models used and from the assumption of complete local thermal equilibrium. When theoretical uncertainties within hydrodynamics are fairly treated, does a convincing signal for a soft EOS survive?

The indirect evidence for a phase transition of some sort in the elliptic flow results comes primarily from the sensitivity in hydrodynamics calculations of the magnitude and hadron mass-dependence of v2 to the EOS. How does the level of this EOS sensitivity compare quantitatively to that of uncertainties in the calculations, gleaned from the range of parameter adjustments and the observed deviations from the combination of elliptic flow, spectra and HBT correlations?

5.2.2 Jet quenching and high gluon density

The parton energy loss treatments do not directly distinguish passage through confined vs. deconfined systems. Evidence of deconfinement must then be indirect, via comparison of the magnitude of inferred gluon or energy densities early in the collision to those suggested by independent partonic treatments such as gluon saturation models. The actual energy loss inferred from fits to

RHIC data, through the rapidly expanding collision matter, is only slightly larger than that indicated through static cold nuclei by fits to semi-inclusive deep inelastic scattering data. The significance of the results is then greatly magnified by the correction to go from the expanding collision matter to an equivalent static system at the time of the initial hard scattering. The quantitative uncertainties listed in the question will then be similarly magnified. What, then, is a reasonable guess of the range of initial gluon or energy densities that can be accommodated, and how does one demonstrate that those densities can only be reached in a deconfined medium?

Does the magnitude of the parton energy loss inferred from RHIC hadron suppression observations demand an explanation in terms of traversal through deconfined matter? The answer must take into account quantitative uncertainties in the energy loss treatment arising, for example, from the uncertain applicability of factorization in-medium, from potential differences (other than those due to energy loss) between in-medium and vacuum fragmentation, and from effects of the expanding matter and of energy loss of the partons through cold matter preceding the hard scattering.

5.3 Have we assumed the answer?

Our understanding of hot dense matter, and of the nuclear EoS is evolving rapidly with new experimental results. The Quark-Gluon Plasma apparently does not behave as we originally believed it would. On its face, this is "discovery physics" at its best, experimentally exploring a new domain.

However, the situation may be viewed in a different light. What we in the field might consider exciting advances in insight, a skeptical outsider might see as revisionism. He might observe that we originally set out to create the QGP, which we would identify via certain signatures in the data (strangeness enhancement, large HBT radii, high entropy, etc).

If large HBT radii, nontrivial structure in $v_2(\sqrt{s_{NN}}$, and/or large entropy were observed, but jet quenching was not observed, would a QGP claim still be made? Does one need only a subset of the expected signatures?

When creation of deconfined matter (though with quite different properties than expected) is claimed in the absence of several signals, the skeptical outsider might ask whether claims of discovery of the QGP would be made *whatever* the data showed.

Such questions naturally arise in light of the unsatisfying but frequently-

expressed statement that "the energy density at RHIC is so high that the matter could not be anything but deconfined." In constrast to the desired model-independent statement, this appears to be almost a *data*-independent statement.

5.3.1 Lack of threshold effects

This issue is related to that of "cross-checks" mentioned above.

The hallmark of QGP formation in lattice QCD calculations, and as sold to the larger physics community for years, is a rapid transition around a critical temperature leading to deconfinement and, quite possibly, chiral symmetry restoration. Can we make a compelling claim to have discovered a new form of matter if we are not yet able to demonstrate convincingly either deconfinement, or chiral restoration, or a rapid transition in some aspect of the collision behavior? If the transition temperature should be reached below RHIC and SPS energies, or in lighter systems or more peripheral collisions, where should it be reached, and how might one see its effects via a non-smooth signal as a function of energy, system size or centrality? Is it conceivable that there is no rapid transition in nature, but just a gradual evolution from dominance of hadronic toward dominance of partonic degrees of freedom? If the latter is the case, is the question of QGP "discovery" well-posed?

Can we make a convincing QGP discovery claim without clear evidence of a phase transition? Can we predict, based on what we now know from SPS and RHIC collisions, at what energies or under what conditions we might produce matter below the critical temperature, and which observables from those collisions should not match smoothly to SPS and RHIC results?

5.3.2 Is the EoS known? Do we simply need more computing power?

One response to the question posed in Section 5.2.1 is that EOS is already known from lattice QCD calculations, so that only the degree of thermalization is open to doubt. Such a view tends to trivialize the QGP search by presuming the answer.

An original motivation for the experimental program at RHIC was to explore the QCD Equation of State (EoS). Indeed, many early talks to the community at large began with statements to the effect that "QCD is *believed* to be the theory of the strong interaction, and the RHIC experimental program is necessary to test the nonperturbative regime."

If lattice calculations are taken as necessarily correct, so that, e.g. one cannot validly vary the EoS in model calculations, what then is the purpose of the RHIC experimental program?

Though lattice calculations are presently unable to explore the full phasespace of QCD, these issues are generally viewed as technical. Diverting resources from the experimental to the lattice program would likely help solve these technical issues.

Responding that its purpose is to search for new phenomena not theoretically understood allows that lattice may not be the whole story, and that trying other Equations of State is a valid and necessary exercise.

6 Overview and Outlook

6.1 What have we learned from the first three years of RHIC measurements?

Already in their first three years, all four RHIC experiments have been enormously successful in producing large volumes of high-quality data illuminating the dynamics of heavy-ion collisions in a new regime of very high energy densities. In parallel, there have been significant advances in the theoretical treatment of these collisions. A number of the most striking features of RHIC experimental results have been described to a reasonable quantitative level, and in some cases even predicted beforehand, using theoretical treatments inspired by QCD and based on QGP formation in the early stages of the collisions.

The observed hadron spectra and correlations at RHIC reveal three transverse momentum ranges with distinct behavior: a soft range ($p_T \lesssim$1.5 GeV/c) containing the vast majority of produced hadrons, representing most of the remnants of the bulk collision matter; a hard range ($p_T \gtrsim$ 6 GeV/c), providing partonic probes of the early collision matter; and an intermediate, or firm, range (1.5 $\lesssim p_T \lesssim$ 6 GeV/c). The behavior in each of these ranges is quite different than would be expected from an incoherent sum of independent nucleon-nucleon collisions. Below we summarize the major findings described in earlier chapters within each of these three ranges, in each case listing them in approximate decreasing order of what we judge to be their level of robustness with respect to current experimental and theoretical ambiguities. This is not intended necessarily to represent order of importance, as some of the presently model-dependent conclusions are among the strongest arguments in favor of QGP formation.

6.1.1 Soft sector

- The matter produced exhibits **strong collective flow**: most hadrons at low p_T reflect a communal transverse velocity field resulting from conditions early in the collision, when the matter was clearly expanding rapidly under high, azimuthally anisotropic, pressure gradients and frequent interactions among the constituents. The commonality of the velocity is clearest from the systematic dependence of elliptic flow strength on hadron mass at low p_T (see Fig. 18), from the common radial flow velocities extracted by fitting observed spectra (Fig. 14), and from the measurements of HBT and non-identical particle correlations [117]. All of these features fit naturally, at least in a qualitative way, within a hydrodynamic description of the system evolution.

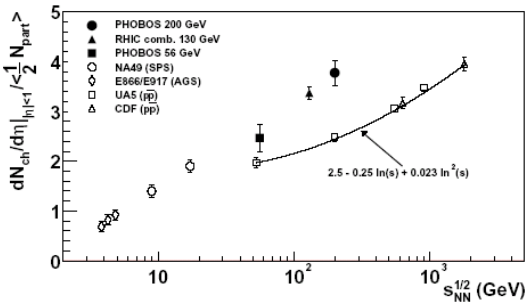

Fig. 26. *Measured mid-rapidity charged particle densities, scaled by the calculated number of participant nucleons, for central collisions of $A \sim 200$ nuclei at AGS, SPS and RHIC, plotted as a function of the center-of-mass energy. Results for $\overline{p}+p$ collisions are shown for comparison. Figure from [59].*

- In the soft sector, most bulk properties measured appear to fall on quite smooth curves with similar results from lower-energy collisions. Examples shown include charged particle density (Fig. 26), elliptic flow (Fig. 27), and freezeout radii inferred from HBT analyses (Fig. 28). Similarly, the centrality-dependences observed at RHIC are smooth. **We have thus not yet found any "smoking-gun" signal for a rapid transition in the nature of the collision matter produced**, of the type originally anticipated [2].
- Despite the smoothness of the energy and centrality dependences, two important milestones related to the attainment of thermal equilibrium appear to be reached for the first time in central full-energy RHIC collisions. The first is that **the yields of different hadron species, *up to and including multi-strange hadrons*, become consistent with a Grand Canonical statistical distribution** at a chemical freezeout temperature of 160 ± 10 MeV and a baryon chemical potential ≈ 25 MeV (see Fig. 12). This result places an effective lower limit on the temperatures attained if thermal equilibration is reached during the collision stages preceding this freezeout. This lower limit is **close to the QGP transition temperature predicted by lattice QCD calculations** (see Fig. 1).
- At the same time (*i.e.*, for near-central full-energy collisions) the mass- and p_T-dependence of the observed hadron spectra and of the strong elliptic flow in the soft sector become **consistent, at the $\pm 20-30\%$ level, with hydrodynamic expectations for an *ideal* relativistic fluid** formed with an initial eccentricity characteristic of the impact parameter. These hydrodynamic calculations have not yet succeeded in also quantitatively explaining the emitting shape at freezeout, inferred from measured HBT correlations (see Fig. 20). Nonetheless, their overall success suggests that the interactions among constituents in the initial stages of these near-central collisions are characterized by very short mean free paths, leading to **quite rapid ($\tau \lesssim 1$ fm/c) attainment of at least approximate local ther-**

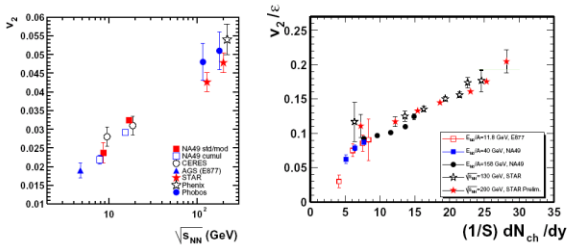

Fig. 27. *(a) Energy dependence of elliptic flow measured near mid-rapidity for mid-central collisions ($\sim 12-34\%$ of the geometric cross section) of $A \sim 200$ nuclei at the AGS, SPS and RHIC. (b) Mid-rapidity elliptic flow measurements from various energies and centralities combined in a single plot of v_2 divided by relevant initial spatial eccentricity vs. charged-particle rapidity density per unit transverse area in the $A-A$ overlap region. The figures, taken from Ref. [118], highlight the smooth behavior of flow vs. energy and centrality. The rightmost points represent central to mid-central STAR results, where the observed v_2/ϵ ratio becomes consistent with hydrodynamic expectations for an ideal relativistic fluid.*

mal equilibrium. The short mean free path in turn suggests a very dense initial system.

- Based on the rapid attainment of thermal equilibrium, and making the assumption of longitudinal boost-invariant expansion, one can extract [114] a lower bound on the initial energy density from measured rapidity densities [115] of the total transverse energy (dE_T/dy) produced in the collisions. These estimates suggest that in central Au+Au collisions at RHIC, **matter is formed at an initial energy density well above the critical density** ($\sim 0.5-1.0$ GeV/fm^3) predicted by LQCD for a transition to the QGP.
- Hydrodynamics calculations are best able to reproduce RHIC results for hadron spectra and the magnitude and mass-dependence of elliptic flow (Fig. 18) by utilizing **a relatively soft Equation of State, incorporating an LQCD-inspired phase transition from QGP to hadronic matter**. However, the calculations also exhibit strong sensitivity to other *a priori* unknown features, namely, the details of the hadronic final-state interactions preceding chemical freezeout and the time at which thermal equilibrium is first attained. In light of these competing sensitivities, it is not yet clear if the experimental results truly *demand* a soft EOS.

6.1.2 Firm sector

- In the intermediate p_T range, the elliptic flow strength v_2 saturates and we see systematic meson vs. baryon differences (rather than a systematic mass-dependence) in both yield (see Fig. 15) and v_2 value (Figs. 19). In the same region we also observe clear jet-like angular correlation peaks in the near-side azimuthal difference distributions between pairs of hadrons (see Fig. 23). The most natural interpretation for this combination of character-

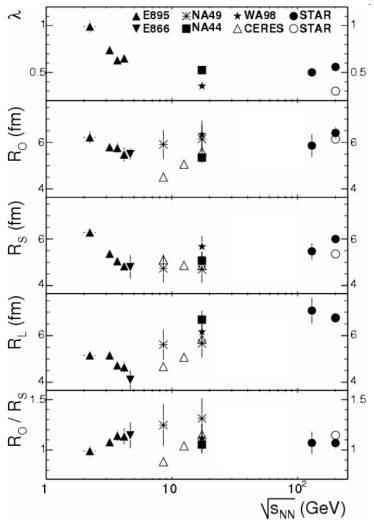

Fig. 28. *Energy dependence of HBT parameters extracted from pion pair correlations in central $A-A$ ($A \sim 200$) collisions at mid-rapidity and pair $k_T \approx 0.2$ GeV/c. The data span the AGS, SPS and RHIC.*

istics is that **the firm yield arises from a mixture of partonic hard-scattering (responsible for the jet-like correlations) and softer (responsible for the meson-baryon differences) processes**.

- **The v_2 values appear to scale with the number of constituent quarks n in the hadron studied**, *i.e.*, v_2/n vs. p_T/n falls on a common curve for mesons and baryons (see Fig. 19). This scaling works surprisingly well, but cannot be strictly valid, at low p_T, where the flow measurements reveal a clear mass-dependence (see Fig. 18). But the scaling is consistent with the so far limited particle-identified data for the v_2 saturation values. If this trend persists as the data are improved, it would provide direct experimental evidence for the relevance of constituent quark degrees of freedom in the hadronization process, and in determining flow for firm hadrons, in RHIC collisions.
- Quark recombination models are able to fit the observed meson and baryon spectra in the firm sector by **a sum of contributions from coalescence of thermalized constituent quarks following an exponential p_T spectrum and from fragmentation of initially hard-scattered partons with a power-law spectrum** [53]. It is not yet clear if the same mixture can also account quantitatively for the v_2 (whose scaling suggests the coalescence contribution alone) and azimuthal dihadron correlation (including background under the jet-like peaks) results as a function of p_T.

6.1.3 Hard sector

- The dominant characteristic of the hard regime is **the strong suppression of hadron yields in central Au+Au collisions**, in comparison to expectations from p+p or peripheral Au+Au collisions, scaled by the number of contributing binary (nucleon-nucleon) collisions (see Fig. 25). Such suppression sets in already in the firm sector, but saturates and remains constant as a function of p_T throughout the hard region explored to date. Such suppression was not seen in d+Au collisions at RHIC, indicating that it is **a final-state effect associated with the collision matter produced in Au+Au**. It is consistent with effects of parton energy loss in traversing dense matter, predicted before the data were available [106,107].
- Azimuthal correlations of firm with firm (see Fig. 23) and of hard with firm [104] hadrons exhibit clear jet-like peaks on the near side. However, **the anticipated away-side peak associated with dijet production is suppressed** by progressively larger factors as the Au+Au centrality is increased, and for given centrality, as the amount of (azimuthally anisotropic) matter traversed is increased (see Fig. 23). Again, no such suppression is observed in d+Au collisions. The suppression of hadron yields and back-to-back correlations firmly establish that **jets are quenched by very strong interactions with the matter produced in central Au+Au collisions**. The jet-like near-side correlations survive presumably because one observes preferentially the fragments of partons scattered outward from the surface region of the collision zone.
- Most features of the observed suppression of high-p_T hadrons, including the centrality-dependence and the p_T-independence, can be described efficiently by **perturbative QCD calculations incorporating parton energy loss** in a thin, dense medium (see Fig. 25). To reproduce the magnitude of the observed suppression, despite the rapid expansion of the collision matter the partons traverse, these treatments need to assume that **the initial gluon density when the collective expansion begins is at least an order of magnitude greater than that characteristic of cold, confined nuclear matter** [106]. The inferred gluon density is consistent, at a factor ~ 2 level, with the saturated densities needed to account for RHIC particle multiplicity results in gluon saturation models (see Fig. 11).
- Angular correlations between firm and soft hadrons have been used to explore how transverse momentum balance is achieved, in light of jet quenching, opposite a high-p_T hadron in central Au+Au collisions. The results (see Fig. 24) show the balancing hadrons to be significantly larger in number, softer and more widely dispersed in angle compared to p+p or peripheral Au+Au collisions, with **little remnant of away-side jet-like behavior**. To the (not yet clear) extent that hard scattering dominates these correlations, the results could signal an approach of the away-side parton toward thermal equilibrium with the bulk matter it traverses.
- The hard sector was not accessible in SPS experiments, so any possible

energy dependence of jet quenching can only be explored via the hadron nuclear modification factor in the firm sector. The results (see Fig. 29) leave open the possibility of a rapid transition, though serious questions have been raised [119] about the validity of the p+p reference data used to determine the SPS result in the figure.

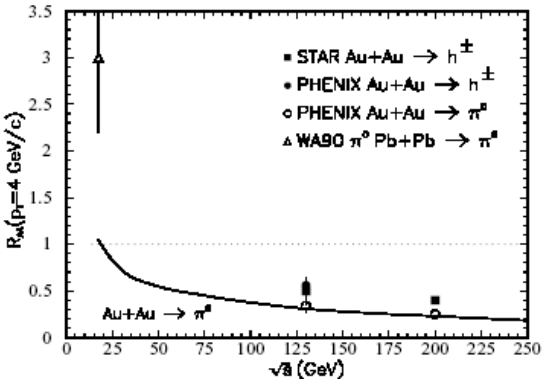

Fig. 29. *The nuclear modification factor measured for 4 GeV/c hadrons in central $A - A$ ($A \sim 200$) collisions at SPS and two RHIC energies, showing (Cronin) enhancement at the lower energy and clear jet-quenching suppression at RHIC. The small difference between RHIC charged hadron and identified π^0 results reflects meson vs. baryon differences in this p_T range. The solid curve represents a parton energy loss calculation under simplifying assumptions concerning the energy-dependence, as described in [106].*

In summary, the RHIC program has enabled major advances in the study of hot strongly interacting matter, for two basic reasons. With the extended reach in initial energy density, the matter produced in the most central RHIC collisions appears to have attained conditions that considerably simplify its theoretical treatment: essentially ideal fluid expansion, and approximate local thermal equilibrium beyond the LQCD-predicted threshold for QGP formation. With the extended reach in particle momentum, the RHIC experiments have developed probes for behavior that was inaccessible at lower collision energies: jet quenching and apparent constituent quark scaling of elliptic flow. These results indicate, with fairly modest reliance on theory, that RHIC collisions produce highly dissipative and dense matter that behaves collectively.

If one takes seriously all of the theoretical successes mentioned above, they suggest the following emerging overall picture of RHIC collisions: Interactions of very short mean free path within the gluon density saturation regime lead to a rapidly thermalized partonic system at energy densities and temperatures above the LQCD critical values. This thermalized matter expands collectively and cools as an ideal fluid, until the phase transition back to hadronic matter begins, leading to a significant pause in the build-up of elliptic flow. During and after the phase transition, constituent quarks appear to emerge as the effective degrees of freedom in describing hadron formation at medium p_T

out of this initially partonic matter. Initially hard-scattered partons (with lower color interaction cross sections than the bulk partons) traversing this matter lose substantial energy to the medium via gluon radiation, and thereby approach, but do not quite reach, equilibration with the bulk matter. Thus, some evidence of degraded jets survives, depending on the amount of matter traversed. Any claim of QGP discovery based on RHIC results to date requires an assessment of the robustness, internal consistency, quantitative success and predictive power of this emerging theoretical picture.

6.2 Are we there yet?

The consistency noted above of many RHIC results with a QGP-based theoretical framework is an important and highly non-trivial statement! Indeed, it is the basis of some publicized claims [1,120] that the Quark-Gluon Plasma has been "nailed down" at RHIC. In our judgment, there is still cause at this juncture for healthy skepticism about these claims, on several grounds mentioned below, and also reflected in the list of open questions provided in Chap. 5 of this document.

- The RHIC experiments have not yet produced *direct* evidence for deconfinement, for chiral restoration, or indeed for any rapid transition in thermodynamic properties of the matter produced. If the theoretical treatment of RHIC results is robust, it should be capable of now predicting, *without further adjustment of parameters*, whether there are bombarding energies, system sizes and centralities at which heavy-ion collisions might produce thermally equilibrated matter at initial temperatures *below* the predicted critical value, as would be needed to observe a clear rapid transition in some measured properties.
- The indirect evidence for a phase transition and for attainment of local thermal equilibrium in the produced matter are intertwined in the hydrodynamics account for RHIC hadron spectra and elliptic flow results. The uniqueness of the solution involving early thermalization and a soft EOS is not yet demonstrated. Nor is its robustness against changes in the treatment of chemical freezeout, as might be needed, for example, to reduce discrepancies from HBT measurements.
- The indirect evidence for deconfinement rests primarily on the large initial gluon densities inferred from parton energy loss fits to the observed hadron suppression at high p_T. It has not yet been demonstrated that the extracted values *demand* deconfinement in the matter traversed. The agreement with initial gluon densities suggested by Color Glass Condensate approaches is encouraging, but is still at a basically qualitative level.
- The role of collectively flowing constituent quarks as the effective degrees of freedom for hadron formation at intermediate p_T is not yet well established

experimentally. If it becomes so established by subsequent measurements and analyses, this will hint at, but not conclusively demonstrate, the existence of an earlier collective partonic stage in the system evolution. The compatibility of constituent quark scaling of v_2 at low p_T with the hadron mass-dependence that is a hallmark of hydrodynamics has yet to be explained.

- The observed smooth, monotonic nature of the dependence of most soft observables on collision energy and centrality should be accounted for clearly in theoretical calculations. In the emerging picture, matter was probably also formed above or at the critical energy density in SPS collisions, but the distinct stages of its evolution were more blurred by a shorter-lived thermalized partonic state, or perhaps a failure to achieve thermal equilibrium at all.
- The theory remains a patchwork of different treatments applied in succession to each stage of the system evolution. So far, we have assembled five "pillars of wisdom" for RHIC central Au+Au collisions, and each invokes a separate model or theoretical approach for its interpretation: (i) statistical model fits to measured hadron yields to infer possible chemical equilibrium across the u, d and s sectors; (ii) hydrodynamics calculations of elliptic flow to suggest early thermalization and soft EOS; (iii) quark recombination models to highlight the role of thermalized constituent quarks in firm-sector v_2 scaling; (iv) parton energy loss models to infer an initial gluon density from high-p_T hadron suppression observations; (v) gluon saturation model fits to observed hadron multiplicities, to suggest how high-density QCD may predetermine the achieved initial gluon densities. Each piece of the patchwork has its own assumptions, technical difficulties, adjusted parameters and quantitative uncertainties, and they fit together somewhat uneasily. Until they are assimilated into a self-consistent whole with only a few overall parameters fitted to existing data, it may be difficult to assess theoretical uncertainties quantitatively or to make non-trivial quantitative predictions whose comparison with future experimental results have the potential to prove the theory wrong.

The bottom line is that in the absence of a direct "smoking gun" signal of deconfinement revealed by experiment alone, a QGP discovery claim must rest on the comparison with a promising, but still not yet mature, theoretical framework. In this circumstance, clear predictive power with quantitative assessments of theoretical uncertainties are necessary for the present appealing picture to survive as a lasting one.

6.3 What are the critical needs from future experiments?

The above comments make it clear what is needed most urgently from theory. But how can future measurements, analyses and heavy-ion collision facilities bring us to a more definitive conclusion regarding the formation of a Quark-Gluon Plasma, and to a clearer delineation of the fundamental properties of the matter produced? We briefly describe below the goals of some important anticipated programs, separated into short-term and long-term prospects. In the short term, RHIC measurements should concentrate on verifying and extending its new observations of jet quenching and v_2 scaling; on searching for possible signals of a phase transition and testing quantitative theoretical predictions at lower energies and perhaps for different system sizes; and on measuring charmed-hadron and charmonium yields and flow to search for other evidence of deconfinement. Some of the relevant data have already been acquired during the highly successful 2004 RHIC run – which has increased the RHIC database by an order of magnitude – and simply await analysis, while other measurements require anticipated near-term upgrades of the detectors. In the longer term, the LHC will become available to provide crucial tests of QGP-based theoretical extrapolations to much higher energies, and to focus on very high p_T probes of collision matter that is likely to be formed deep into the gluon saturation regime. Over that same period, RHIC should provide the extended integrated luminosities and upgraded detectors needed to undertake statistically challenged measurements to probe directly the initial system temperature, the fate of strong-interaction symmetries in the early collision matter, and the quantitative energy loss of partons traversing that matter.

Important short-term goals include the following:

- **Establish v_2 scaling more definitively.** Extend the particle-identified flow measurements for hadrons in the medium-p_T region over a broader p_T range, a wider variety of hadron species, and as a function of centrality. Does the universal curve of v_2/n vs. p_T/n remain a good description of all the data? How is the scaling interpretation affected by anticipated hard contributions associated with differential jet quenching through spatially anisotropic collision matter? Can the observed di-hadron angular correlations be quantitatively accounted for by a 2-component model attributing hadron production in this region to quark coalescence (with correlations reflecting only the collective expansion) plus fragmentation (with jet-like correlations)? Do hadrons such as ϕ-mesons or Ω-baryons, containing no valence u or d quarks, and hence with OZI-suppressed hadronic interaction cross sections in normal nuclear matter, follow the same flow trends as other hadrons? Do the measured v_2 values for resonances reflect their constituent quark, or rather their hadron, content? These investigations have the poten-

tial to establish more clearly that constituent quarks exhibiting collective flow are the relevant degrees of freedom for hadronization at medium p_T.

- **Establish that jet quenching is an indicator of parton, and not hadron, energy loss.** Extend the measurements of hadron energy loss and di-hadron correlations to higher p_T, including particle identification in at least some cases. Do the meson-baryon suppression differences seen at lower p_T truly disappear? Does the magnitude of the suppression remain largely independent of p_T, in contrast to expectations for hadron energy loss [39]? Does one begin to see a return of away-side jet behavior, via punch-through of correlated fragments opposite a higher-p_T trigger hadron? Improve the precision of di-hadron correlations with respect to the reaction plane, and extend jet quenching measurements to lighter colliding nuclei, to observe the non-linear dependence on distance traversed, expected for radiating partons [34]. Measure the nuclear modification factors for charmed meson production, to look for the "dead-cone" effect predicted [40] to reduce energy loss for heavy quarks.
- **Extend RHIC Au+Au measurements down toward SPS measurements in energy, to search for possible indicators of a phase transition.** The apparent observation of significant *enhancement* of hadron yields at $p_T \approx 4$ GeV/c at SPS energies, in marked contrast to the strong suppression at RHIC energies (see Fig. 29), leaves open the possibility of a rapid onset of jet quenching within the RHIC regime. Ambiguities in the SPS result, associated with flaws in the relevant p+p reference set [119], point out the importance of supplementing A+A measurements at lower collision energies with suitable p+p data. Observation of a rapid transition in hadron suppression would greatly strengthen a QGP discovery claim, while observation of smooth behavior would test quantitative predictions of the gluon saturation and parton energy loss models.
- **Measure charmonium yields and open charm yields and flow, to search for signatures of color screening and partonic collectivity.** Use particle yield ratios for charmed hadrons to determine whether the apparent thermal equilibrium in the early collision matter at RHIC extends even to quarks with mass significantly greater than the anticipated system temperature. From the measured p_T spectra, constrain the relative contributions of coalescence vs. fragmentation contributions to charmed-quark hadron production. Compare D-meson flow to the trends established in the u, d and s sectors, and try to extract the implications for flow contributions from coalescence vs. possibly earlier partonic interaction stages of the collision. Look for the extra suppression of charmonium, compared to open charm, yields expected to arise from the strong color screening in a QGP state (see Fig. 2). Since recent LQCD calculations [8] predict onset of charmonium melting at quite different temperatures above T_c for J/ψ vs. ψ', it is important to identify both particles clearly in the experiments, though ψ' measurements require the detector upgrades and greater integrated luminosity characteristic of the longer-term programs below.

Longer-term prospects, requiring much greater integrated luminosities or substantial facility developments, include:

- **Develop thermometers for the early stage of the collisions, when thermal equilibrium is first established.** In order to pin down experimentally where a phase transition may occur, it is critical to find probes with direct sensitivity to the temperature well before chemical freezeout. Promising candidates include direct photons – measured either singly at high p_T where π^0 background may be manageable, or down to low momentum via $\gamma - \gamma$ HBT, which is insensitive to π^0's – and thermal dileptons, which can be identified using hadron-blind detectors and techniques.
- **Quantify parton energy loss by measurement of mid-rapidity jet fragments tagged by a hard direct photon, a heavy-quark hadron, or a far forward energetic hadron.** Such luminosity-hungry coincidence measurements will elucidate the energy loss of light quarks vs. heavy quarks vs. gluons, respectively, through the collision matter. They should thus provide more quantitative sensitivity to the details of parton energy loss calculations.
- **Test quantitative predictions for elliptic flow in U+U collisions.** The large size and deformation of uranium nuclei make this a considerable extrapolation away from RHIC Au+Au conditions, and a significant test for the details of hydrodynamics calculations that are consistent with the Au+Au results [11].
- **Measure hadron multiplicities, yields, correlations and flow at LHC and GSI energies, and compare to quantitative predictions based on models that work at RHIC.** By fixing parameters and ambiguous features of gluon saturation, hydrodynamics, parton energy loss and quark coalescence models to fit RHIC results, and with guidance from LQCD calculations regarding the evolution of strongly interacting matter with initial temperature and energy density, theorists should make quantitative predictions for these observables at LHC and GSI before the data are collected. The success or failure of those predictions will represent a stringent test of the viability of the QGP-based theoretical framework.
- **Devise tests for the fate of fundamental QCD symmetries in the collision matter formed at RHIC.** If the nature of the QCD vacuum is truly modified above the critical temperature, then chiral and $U_A(1)$ symmetries may be restored, while CP may conceivably be broken [121]. Testing these symmetries in this unusual form of strongly interacting matter is of great importance, even if we do not have a crisp demonstration beforehand that the matter is fully thermalized and deconfined. Approaches that have been discussed to date include looking for meson mass shifts in dilepton spectra as a signal of chiral symmetry restoration, and using $\Lambda - \overline{\Lambda}$ spin correlations to search for CP violation. It may be especially interesting to look for evidence among particles emerging opposite an observed high-p_T hadron tag, since the strong suppression of away-side jets argues that the fate of the

away-side particles may reflect strong interactions with a maximal amount of early collision matter.

It may at first seem disappointing to conclude that advances in theory and experiment are still needed to decide definitively if we have formed a Quark-Gluon Plasma state in RHIC collisions. However, this must be weighed against the very clear progress made in RHIC's first three years in addressing this complex, but profoundly important set of questions regarding the nature of strongly interacting matter and the QCD vacuum. We hope that this assessment has made it clear that the progress is real and extensive, and that the remaining questions are well defined and crisply posed.

References

[1] M. Gyulassy, *nucl-th*/0403032.

[2] J.W. Harris and B. Müller, Annu. Rev. Nucl. Part. Sci. **46**, 71 (1996).

[3] U. Heinz and M. Jacob, *nucl-th*/0002042.

[4] D.H. Rischke, Prog. Part. Nucl. Phys. **52**, 197 (2004).

[5] F. Karsch, *Lecture Notes in Physics* **583**, 209 (2002).

[6] O. Kaszmarek, F. Karsch, E. Laermann and M. Lütgemeier, Phys. Rev. D**62**, 034021 (2000).

[7] T. Matsui and H. Satz, Phys. Lett. B**178**, 416 (1986); F. Karsch, M.T. Mehr and H. Satz, Z. Phys. C **37**, 617 (1988).

[8] M. Asakawa and T. Hatsuda, Phys. Rev. Lett. **92**, 012001 (2004); S. Datta *et al.*, *hep-lat*/0403017.

[9] E. Laermann and O. Philipsen, *hep-ph*/0303042.

[10] Z. Fodor and S.D. Katz, Phys. Lett. B**534**, 87 (2002) and JHEP **0203**, 014 (2002).

[11] P. F. Kolb and U. Heinz, in *Quark Gluon Plasma 3*, eds. R.C. Hwa and X.-N. Wang (World Scientific, Singapore, 2003)and *nucl-th*/0305084.

[12] L.D. Landau, *Izv. Akad Nauk SSSR, ser. fiz* 17 (1953) 51. L.D. Landau and E.M. Lifshitz, "Fluid Mechanics".

[13] E. Shuryak, hep-ph/0312227.

[14] R. Stöck, "Heavy-ion Physics: from Bevalac to LHC", Quark Matter 2004, January 12-17, 2004, Oakland, California.

[15] R. Hagedorn, *Nuovo Cimento* **3**, 1965 (1)47.

[16] S. Bass and A. Dumitru, *Phys. Rev.* C **61**, 064909 (2000).

[17] D. Teaney, J. Lauret, and E. Shuryak, Phys. Rev. Lett. **86**, 47839(2001), and *nucl-th*/0110037.

[18] H. Sorge, Phys. Rev. C **52**, 3291 (1995).

[19] P.F. Kolb, J. Sollfrank and U. Heinz, Phys. Rev. C **62**, 054909 (2000).

[20] P. Huovinen, P.F. Kolb, U. Heinz, P.V. Ruuskanen and S.A. Voloshin, Phys. Lett. B**503**, 58 (2001).

[21] D. Teaney, *Phys. Rev.* C **68**, 034913 (2003).

[22] H. van Hecke, H. Sorge and N. Xu, *Phys. Rev. Lett.* **81**, 5764 (1998).

[23] N. Xu and Z. Xu, *Nucl. Phys.* A **715**, 587c (2003).

[24] B. Tomášik and U.A. Wiedemann, in *Quark Gluon Plasma 3*, eds. R.C. Hwa and X.-N. Wang (World Scientific, Singapore, 2003), and *hep-ph*/0210250.

[25] E. Fermi, *Prog. Theor. Phys.* **5**, 570 (1950).

[26] P. Braun-Munzinger, K. Redlich and J. Stachel, nucl-th/0304013.

[27] P. Braun-Munzinger, J. Stachel, J.P. Wessels and N. Xu, *Phys. Lett.* B **365**, 1 (1)1996.

[28] K. Huang, *Statistical Mechanics*, .

[29] E.V. Shuryak, *Phys. Lett.* B **42**, 1972 (357); J. Rafelski and M. Damos, *Phys. Lett.* B **97**, 1980 (279); R. Hagedorn and K. Redlich *Z. Phys.* C **27**, 541 (1985).

[30] V. Koch, *Nucl. Phys.* A **715**, 108c (2003).

[31] A.M. Poskanzer and S.A. Voloshin, *Phys. Rev.* C **58**, 1671 (1998).

[32] G. Torrieri and J. Rafelski, *Phys. Lett.* B **509**, 239 (2001); Z. Xu, *J. Phys.* G **30**, S325 (2004); M. Bleicher and H. Stocker, *J. Phys.* G **30**, S111 (2004).

[33] J.D. Bjorken, FERMILAB-PUB-82-59-THY and erratum (unpublished).

[34] M. Gyulassy, I. Vitev, X.-N. Wang and B.-W. Zhang, in *Quark Gluon Plasma 3*, eds. R.C. Hwa and X.-N. Wang (World Scientific, Singapore, 2003) and (*nucl-th*/0302077).

[35] M. Gyulassy, P. Levai and I. Vitev, Nucl. Phys. A **661**, 637 (1999); Nucl. Phys. B **571**, 197 (2000); Phys. Rev. Lett. **85**, 5535 (2000); and Nucl. Phys. B **594**, 371 (2001).

[36] E. Wang and X.-N. Wang, Phys. Rev. Lett. **87**, 142301 (2001).

[37] W. Cassing, K. Gallmeister and C. Greiner, Nucl. Phys. A **735**, 277 (2004).

[38] G.R. Farrar, H. Liu, L.L. Frankfurt and M.I. Strikman, Phys. Rev. Lett. **61**, 686 (1988); S.J. Brodsky and A.H. Mueller, Phys. Lett. B**206**, 685 (1988); B.K. Jennings and G.A. Miller, Phys. Lett. B**236**, 209 (1990); Phys. Rev. D **44**, 692 (1991); Phys. Rev. Lett. **69**, 3619 (1992); and Phys. Lett. B**274**, 442 (1992).

[39] X.-N. Wang, Phys. Lett. B**579**, 299 (2004).

[40] M. Djordjevic and M. Gyulassy, *nucl-th*/0302069.

[41] A. Airapetian *et al.* [HERMES Collaboration], Eur. Phys. J. C **20**, 479 (2001); V. Muccifora [HERMES Collaboration], *hep-ex*/0106088.

[42] J.M. Moss *et al.*, *hep-ex*/0109014.

[43] X.-N. Wang and X.-F. Guo, Nucl. Phys. A **696**, 788 (2001); B.-W. Zhang and X.-N. Wang, *hep-ph*/0301195.

[44] Gluon densities extracted from HERA.

[45] A.H. Mueller, Nucl. Phys. B**335**, 115 (1990) and Nucl. Phys. B**572**, 227 (2002).

[46] L.D. McLerran and R. Venugopalan, *Phys. Rev.* D **49**, 2233 (1994).

[47] L.D. McLerran hep-ph/0311028.

[48] E. Iancu and R. Venugopalan, hep-ph/0303204.

[49] D. Kharzeev and M. Nardi, Phys. Lett. **B507**, 121(2001); D. Kharzeev and E. Levin, Phys. Lett. B**523**, 79 (2001).

[50] K.P. Das and R.C. Hwa, *Phys. Lett.* B **68**, 459 (1977); Erratum *ibid.* **73**, 504 (1978); R.G. Roberts, R.C. Hwa and S. Matsuda, *J. Phys.* G **5**, 1043 (1979).

[51] C. Gupt, R.K. Shivpuri, N.S. Verma and A.P. Sharma, *Nuovo Cimento* **75**, 408 (1983); T. Ochiai, *Prog. Theor. Phys.* **75**, 1184 (1986); T.S. Biro, P. Levai and J. Zimanyi, *Phys. Lett.* B **347**, 6 (1995); T.S. Biro, P. Levai and J. Zimanyi, *J. Phys.* G **28**, 1561 (2002).

[52] S.A. Voloshin, *Nucl. Phys.* A **715**, 379c (2003); D. Molnar and S.A. Voloshin, *Phys. Rev. Lett.* **91**, 092301 (2003); R.J. Fries, B. Muller, C. Nonaka and S.A. Bass, *Phys. Rev. Lett.* **90**, 202303 (2003); V. Greco, C.M. Ko and P. Levai, *Phys. Rev. Lett.* **90**, 202302 (2003); Z.W. Lin and C.M. Ko, *Phys. Rev. Lett.* **89**, 202302 (2002); Z.W. Lin and D. Molnar, *Phys. Rev.* C **68**, 044901 (2003).

[53] B. Müller, *nucl-th*/0404015.

[54] C. Adler *et al.* [STAR Collaboration], Phys. Rev. Lett. **89**, 202301 (2002).

[55] W. Reisdorf and H.G. Ritter, Ann. Rev. Nucl. Part. Sci. **47**, 663(1997).

[56] H. Sorge, Phys. Lett. **B402**, 251(1997).

[57] J.-Y. Ollitrault, Phys. Rev. **D46**, 229(1992).

[58] B.B. Back *et al.*, (PHOBOS Collaboration), Phys. Rev. **C65**, 061901R(2002).

[59] B.B. Back *et al.*, (PHOBOS Collaboration), nucl-ex/0301017.

[60] J. Adams, *et al.*, (STAR Collaboration), Phys. Rev. Lett. **92**, 112301(2004); nucl-ex/0310004.

[61] H. Sorge, Phys. Rev. Lett. **82**, 2048(1999).

[62] S.S. Adler, *et al.*, (PHENIX Collaboration), Phys. Rev. Lett. **91**, 18301(2003)

[63] J. Adams *et al.* (STAR Collaboration), Phys. Rev. Lett. **92**, 052302(2004); nucl-ex/0306007.

[64] P. Huovinen, private communications, 2003.

[65] X. Dong *et al*, nucl-th/0403030.

[66] J. Castillo, *et al.*, (STAR Collaboration), nucl-ex/0403027.

[67] S.S. Adler, *et al.*, (PHENIX Collaboration), Phys. Rev. **C69**, 034909(2004); nucl-ex/0307022.

[68] E. Yamamoto, *et al.*, (STAR Collaboration), Nucl. Phys. **A715**, 466c(2003).

[69] K. Schweda, *et al.*, (STAR Collaboration), nucl-ex/0403032.

[70] E. Schnedermann, J. Sollfrank, and U. Heinz, Phys. Rev. **C48**, 2462(1993).

[71] P. Braun-Munzinger, J. Stachel, J. Wessels, and N. Xu, Phys. Lett. **B344**, 43(1995); P. Braun-Munzinger, I. Heppe, and J. Stachel, Phys. Lett. **B465**, 15(1999).

[72] J. Adams *et al.*, (STAR Collaboration), Phys. Rev. Lett., **92**, 182301(2004); nucl-ex/0307024.

[73] H. van Hecke, H. Sorge, and N. Xu, Phys. Rev. Lett., **81**, 5764(1998).

[74] A.M. Poskanzer and S.A. Voloshin, Phys. Rev. C**58**, 1671 (1998).

[75] CERES $v_2(p_T)$ data.

[76] NA49 $v_2(p_T)$ data.

[77] C. Adler, *et al.* (STAR Collaboration), Phys. Rev. Lett. **87**, 182301 (2001).

[78] C. Adler, *et al.* (STAR Collaboration), Phys. Rev. Lett. **87**, 082301 (2001); K. Adeox, *et al.* (PHENIX Collaboration), Phys. Rev. Lett. **88**, 242301 (2002).

[79] J. Adams, *et al.* (STAR Collaboration), Phys. Rev. Lett. **92**, 062301 (2003).

[80] For general introduction of two-particle correlation studies, see U.A. Wiedemann and U. Heinz, Phys. Rep. **319**, 145(1999); B. Jacak and U. Heinz, Ann. Rev. Nucl. Part. Sci. **49**, 529(1999).

[81] G. Bertsch, Nucl. Phys. **A498**, 173c(1989).

[82] D. Rischke and M. Gyulassy, Nucl. Phys. **A597**, 701(1996); *idbd*, Nucl. Phys. **A608**, 479(1996) .

[83] S. Soff, nucl-th/0204040; D. Zschiesche, S. Schramm, H. Stoecker, and W. Greiner, Phys. Rev. **C65**, 014902(2002); S. Soff, S. Bass, and A. Dumitru, Phys. Rev. Lett. **86**, 3981(2001); nucl-th/0012085.

[84] C.Y. Wong, hep-ph/0403025.

[85] M. Stephanov, K. Rajagopal, and E. Shuryak, Phys. Rev. lett. **81**, 4816(1998).

[86] S. Voloshin, V. Koch, and H.G. Ritter, Phys. Rev. **C60**, 024901(1999).

[87] S. Jeon and V. Koch, Phys. Rev. Lett. **85**, 2076(2000).

[88] M. Asakawa, U. Heinz, and B. Müller, Phys. Rev. Lett. **85**, 2072(2000).

[89] S. Bass, P. Danielewicz, and S. Pratt, Phys. Rev. Lett. **85**, 2689(2000).

[90] Q. Liu and T. Trainor, Phys. Lett. **B567**, 184(2003).

[91] M. Gaździcki and St. Mroówczyński, Z. Phys. **C26**, 127(1999).

[92] J. Adams, *et al.*, (STAR Collaboration), Phys. Rev. Lett. **90**, 172301(2003).

[93] A. Bialas, Phys. Lett. **B579**, 31(2004).

[94] J. Adams, *et al.*, (STAR Collaboration), Phys. Rev. **C68**, 044905(2003).

[95] J. Adams, *et al.*, (STAR Collaboration), nucl-ex/0308033.

[96] G. Westfall, (STAR Collaboration), nucl-ex/0404004.

[97] I. Arsene, *et al.*, (BRAHMS Collaboration), Phys. Rev. Lett. **91**, 072305 (2003).

[98] S.S. Adler, *et al.*, (PHENIX Collaboration), Phys. Rev. Lett. **91**, 072303 (2003).

[99] B.B. Back, *et al.*, (PHOBOS Collaboration), Phys. Rev. Lett. **91**, 072302 (2003).

[100] J. Adams, *et al.*, (STAR Collaboration), Phys. Rev. Lett. **91**, 072304 (2003).

[101] C. Adler, *et al.*, (STAR Collaboration), Phys. Rev. Lett. **90**, 082302 (2003).

[102] A.H. Tang, *nucl-ex*/0403018.

[103] K. Filimonov, *nucl-ex*/0403060.

[104] D. Hardtke, Nucl. Phys. A**715**, 272 (2003).

[105] F. Wang, *et al.*, (STAR Collaboration), nucl-ex/0404010.

[106] X.-N. Wang, *nucl-th*/0305010.

[107] I. Vitev and M. Gyulassy, Phys. Rev. Lett. **89**, 252301 (2002).

[108] D. Kharzeev, E. Levin and L. McLerran, Phys. Lett. B**561**, 93 (2003).

[109] J. Adams, *et al.*, (STAR Collaboration), Phys. Rev. Lett. **91**, 172302 (2003).

[110] T. Falter and U. Mosel, Phys. Rev. C**66**, 024608 (2002).

[111] K. Gallmeister, C. Greiner and Z. Xu, Phys. Rev. C**67**, 044905 (2003).

[112] W. Cassing, K. Gallmeister and C. Greiner, Nucl. Phys. A**735**, 277 (2004).

[113] B.B. Back, *et al.*, (PHOBOS Collaboration), Phys. Rev. Lett. **88**, 022302 (2002).

[114] J.D. Bjorken, Phys. Rev. D**27**, 140 (1983).

[115] K. Adcox, *et al.*, (PHENIX Collaboration), Phys. Rev. Lett. **87**, 052301 (2001).

[116] CERES away-side broadening paper.

[117] J. Adams, *et al.*, (STAR Collaboration), Phys. Rev. Lett. **91**, 262302 (2003).

[118] C. Alt, *et al.*, (NA49 Collaboration), Phys. Rev. C**68**, 034903 (2003).

[119] D. d'Enterria, *nucl-ex*/0404018.

[120] RBRC volume: *Discovery of the Strongly Interacting Quark-Gluon Plasma at RHIC*

[121] D. Kharzeev, *et al.*, Phys. Rev. Lett. **81**, 512 (1998).